Utrecht University

KWR

Master's Thesis – Water Science and Management

Preventing hydrological drought in the Pleistocene uplands

A modeling experiment with nature and managed aquifer recharge

Clara Daldegan Balduino (6451578)
c.daldeganbalduino@students.uu.nl
06 8366-7974

UU supervisor: Niko Wanders

Internship Company: KWR Water Research Institute
Supervisor: Marjolein van Huijgevoort
Marjolein.van.Huijgevoort@kwrwater.nl

Word count: 12.980

23/07/2020

Summary

The summer of 2018 has been noted as one of the driest in the current history of the Netherlands. Its effects were widespread, impacting several sectors and water management infrastructure. Despite the above average rainfall in most of the country during the autumn of 2019, areas in the Pleistocene uplands (the sandy elevated regions in the Netherlands) did not reach the required amounts to supply sufficient groundwater recharge in the region and compensate for the 2018 hydrological drought. The scopes of this thesis were to study the effects of managed aquifer recharge (MAR) for hydrological drought prevention in the context of the Pleistocene uplands and determine how much effect it has in alleviating drought stress of agricultural and natural areas. The research question guiding the thesis was *What are the regional effects of locally applied managed aquifer recharge as a measure to prevent hydrological drought and its impacts on natural and agricultural ecosystems in the Pleistocene uplands of the Netherlands?*

After the general characteristics of the Pleistocene uplands were sketched, a theoretical conceptual model was made based on the Achterhoek region of the Netherlands, an area which represents these characteristics well. Next, a combined groundwater (MODFLOW) and a soil-vegetation-atmosphere (MetaSWAP) model was built in iMOD version 5.0. The hypothetical model spanned a region of 15 km long and 15 km wide, where a steady-state model was run and three transient scenarios were applied in a modeling experiment. The 13 scenarios represented different strategies in dealing with hydrological droughts, where the first was a baseline (do nothing) scenario. Two batches of six scenarios applied MAR through the use of injection wells. For one batch (AG MAR) the wells were located at the higher elevation area of the model, and for the second (N MAR) the wells were located at the lower elevation area, about 2 km from the river. Each batch consisted of treatments with different recharge amounts per well (500 m^3/d, 5000 m^3/d and 10000 m^3/d) and each treatment consisted of MAR application in either the summer or winter. Calibration of the model was done based on its steady state simulation, while the validation was done by comparing the normalized groundwater level time series of the baseline scenario and actual groundwater data in the region taken from the DINOloket database. The groundwater level and relative transpiration of each scenario were observed at 12 different locations.

The results show that MAR did have regional effects in preventing hydrological drought and, to a lesser degree in increasing relative transpiration. In general, N MAR scenarios had more widespread effects than AG MAR scenarios, except for the 500 m^3/d treatments, the which effects were too small to be noticed. On the other hand, AG MAR scenarios provided greater groundwater level increase except for where the influence of the river was strongest. In addition, because of the higher groundwater levels, AG MAR also resulted in higher transpiration increase in the area closer to the injection wells than N MAR, as well as a greater overall regional effect in transpiration increase.

Assumptions were made in the model design and in the analysis methods. However the results are conclusive and comparable to literature on MAR measures for hydrological drought prevention and transpiration increase. Recommendations for future research include studying the effects of MAR in a model with the presence of groundwater drainage and to study the combined effects of MAR with the increase of drainage levels in the Pleistocene uplands. Coupled to this combination is the need for restoration of nature areas near rivers and at seepage zones, where often agriculture is practiced and intense drainage occurs. Therefore, the policy recommendation given by this thesis is to apply MAR not only as a stand-alone technical solution, but within a process of land use planning in order to maximize the retention of groundwater and better prevent the impacts of drought.

Table of Contents

Summary 0
1. Introduction 1
2. Conceptual framework 2
2.1 Definitions: propagation of drought 2
2.2 The use of Managed Aquifer Recharge for increasing water availability 4
2.3 Modeling as an approach for experimental research on hydrological drought 4
3. Materials and methods 5
3.1 Description of the Pleistocene uplands 5
3.2 Conceptual Model 6
3.3 Model setup 8
3.4 Model analysis methods 13
4. Results 14
4.1 Steady state model 14
4.2 Baseline scenario 16
4.2.1 Groundwater 16
Model validation 16
Groundwater Results 17
Groundwater contribution to the river 18
4.2.2 Unsaturated zone and vegetation 18
4.3 MAR scenarios 20
4.3.1 The regional effects of locally applied managed aquifer recharge for hydrological drought prevention 20
4.3.2 Effects of MAR on the vegetation 26
5. Discussion and recommendations 33
Assumptions and model simplifications 33
Drought characterization 33
River boundary conditions 34
Drainage conditions 34
Soil representation 34
Comparison to existing MAR studies – Impact on groundwater levels 35
Comparison to existing MAR studies – Impact on vegetation 35
Potential for future MAR applications 35
Impact on land use 36
Human influence drainage 36
6. Conclusion 37
References 38

Appendices 43

1. Introduction

The summer of 2018 has been noted as one of driest in the current history of the Netherlands, but the year started out with above average precipitation, Rhine River discharges (Kramer et al., 2019) and groundwater levels (H2O, 2018; rtv Oost, 2018). Then, in four months' time, precipitation, discharges and groundwater levels decreased significantly, going from extremely wet at the onset of the drought in June 2018, to extremely dry by the end of July. What started out as a meteorological drought due to precipitation deficiencies and evapotranspiration excesses, quickly became a hydrological drought (Eertwegh et al., 2019; Kramer et al., 2019). Hydrological drought is characterized by low surface water discharges and groundwater levels (van Loon, 2015).

The effects of the 2018 drought were widespread, impacting agriculture, shipping, natural ecosystems, drinking water production, recreation, industry, energy production, cities and water management infrastructure (Eertwegh et al., 2019; van Hussen et al., 2020). According to a report commissioned by the Ministry of Infrastructure and Water Management (van Hussen et al., 2020), the total estimated economic damages for these sectors amounted from 450 million to 2.08 billion euros in 2018 alone. The highest quantified costs were in the agricultural sector, followed by the shipping sector and the Dutch water management authorities. These economic losses show only an image of the impacts suffered as a result of the intensely dry summer of 2018, not accounting for the total economic damages suffered in 2019 (van Hussen et al., 2020) and the unquantifiable impacts in the natural and social systems.

The hydrological drought did not quickly abate. Two rainy autumn and winter seasons were needed to compensate for the dry summer of 2018 in most places in the Netherlands, and by 17 December 2019 there were regions where groundwater levels were still below normal (KNMI, 2019a). Despite the above average rainfall in most of the country during the autumn of 2019, areas in the Pleistocene uplands (the sandy elevated regions in the Netherlands) have not reached the required amounts to supply sufficient groundwater recharge in the region and compensate for the 2018 drought (Kramer et al., 2019).

But what causes significant interest is the rapid onset of the hydrological drought from above average wet conditions. Besides the large precipitation deficiency, a plausible reason for this turn of events is the standard operation of water management in the Netherlands. This is focused on draining water to the sea as quickly and efficiently as possible (Eertwegh et al., 2019). Nevertheless, as a result of previous droughts and climate change predictions, Dutch water managers have been changing from a paradigm where a large water runoff and discharge policy is seen as 'safe' to seeing it as 'waste' (IenM, 2015).

During and after the 2018 dry summer, the different types of measures applied by the national and provincial governments and water authorities include saving, accumulating, and supplying water (Eertwegh et al., 2019). A category of measures which can be applied to store water for dry periods and to restore groundwater levels is managed aquifer recharge (MAR), a widely researched array of techniques especially in countries where freshwater is scarce (Dillon et al., 2018).

In a more general sense, MAR is used to actively support the management of groundwater at the local and basin level. Its aim is to improve the efficient use of groundwater, to provide a buffer for hydrological drought and to protect or improve groundwater quality (Stefan & Ansems, 2018). These techniques have been used for centuries around the world for different reasons, but over the last century they have been explicitly used for increasing water storage (Dillon et al., 2018).

In the Netherlands, MAR has been researched and applied for drinking water production (Stefan & Ansems, 2018), thermal energy storage (Fleuchaus et al., 2018) and storing water in saline aquifers

(Sprenger et al., 2017). In addition, there has been recent research on the effects of MAR techniques for the sustainable management of ecosystems and agriculture. As reported by van Loon and others (2014), different possibilities for accumulating water were identified for unconfined aquifers in the Stippelberg forests during the winter months. These included decreasing water losses through diminishing evapotranspiration by slightly decreasing the forest cover, increasing water levels in surface water bodies, or infiltrating water into the more superficial unconfined aquifer, all of which seemed to provide good results in increasing water storage in the subsurface. This project is an example of where MAR techniques and management of the natural environment come into play together, but it still indicates that there is yet much to be researched.

From the Stippelberg project questions still remain regarding the effectiveness of aquifer recharge measures and their role for natural and agricultural areas. In addition, there has generally been little research done on hydrological drought management and prevention, since most of the focus has been on understanding its mechanisms, causes and impacts (Hasan et al., 2019). This knowledge gap provides the scene for the broader purpose of this thesis, which is to contribute to the field of research of MAR as a potential measure for hydrological drought prevention. For this reason the scope of this thesis was to study the effects of MAR for hydrological drought prevention in the context of the Pleistocene uplands and determine how much effect it has in alleviating drought stress of agricultural and natural areas. Consequently, the research question was:

What are the regional effects of locally applied managed aquifer recharge as a measure to prevent hydrological drought and its impacts on natural and agricultural ecosystems in the Pleistocene uplands of the Netherlands?

The sub-questions below guide the research into answering the central question:

1. What are the effects of locally applied managed aquifer recharge through injection wells on regional groundwater levels and channel baseflow?
2. What are the effects of this measure on transpiration in natural and agricultural ecosystems?

Considering the need for climate change adaptation in the densely populated country that is the Netherlands, the current thesis is relevant for society and decision makers. It is relevant for the scientific community, considering the interaction between land use and MAR systems. Furthermore, it is of interest to KWR water research institute, where this thesis was carried out, as it contributes to ongoing projects on drought in the Pleistocene uplands of the Netherlands.

2. Conceptual framework

2.1 Definitions: propagation of drought

Droughts are a natural phenomenon and have impacted humans for several millennia, especially in semi-arid regions. There are still questions on whether climate change will induce an overall drought trend increase in the world. Studies for Europe, however, more relevant for this thesis, show that there is a tendency in increasing extreme events, including drought (IPCC, 2014; Samaniego et al., 2018; Sari Kovats et al., 2014; Wanders et al., 2015). In addition, it is clear that the continent is at high risk of facing water restrictions (IPCC, 2014), making it vulnerable to drought should it occur (Sari Kovats et al., 2014).

Droughts are a natural phenomenon cause by below normal water availability and have affected human water interactions. However, climate change will induce an overall drought trend increase in the world, including Europe (IPCC, 2014; Marx et al., 2018; Samaniego et al., 2018; Sari Kovats et al., 2014; Van Lanen et al., 2018; Wanders et al., 2015; Wanders & Van Lanen, 2015; Wiel et al., 2019). Recently,

Philips et al (2020) also found that consistent trends in drought exist for the interior parts of the Netherlands as a result of climate change.

There are four types of drought (Figure 1) (van Loon, 2015, p. 363) that occur in progression, often termed drought propagation (Mishra & Singh, 2010; Peters, 2003; van Loon, 2015; Wilhite, 2005). Firstly, a lack of sufficient precipitation, named meteorological drought, is caused by anomalies in spatial and temporal rainfall patterns. Meteorological drought occurs when precipitation is below a specified threshold level, considered as the mean climatological precipitation for a given temporal interval (Peters & van Lanen, 2000). A deficit in precipitation coupled to unusually high temperatures leads to soil moisture drought (van Loon, 2015). As a result of less water in the soil and lack of precipitation, there is less water available for runoff to surface waters and percolation into the aquifer. Consequently, low flows in streams and rivers as well as low groundwater levels develop, at which point hydrological drought has been reached.

Soil moisture drought together with hydrological drought cause socio-economic drought leading to socio-economic impacts (Mishra & Singh, 2010; van Loon, 2015) due to a lack of water resources for human activities (Alvarez & Estrela, 2000). Although not treated explicitly in this drought propagation framework, the environment is equally impacted, since a decrease in water availability also affects ecological functions. It is important to note that the further down in drought propagation, the longer it takes to recover (Peters & van Lanen, 2000; van Loon, 2015).

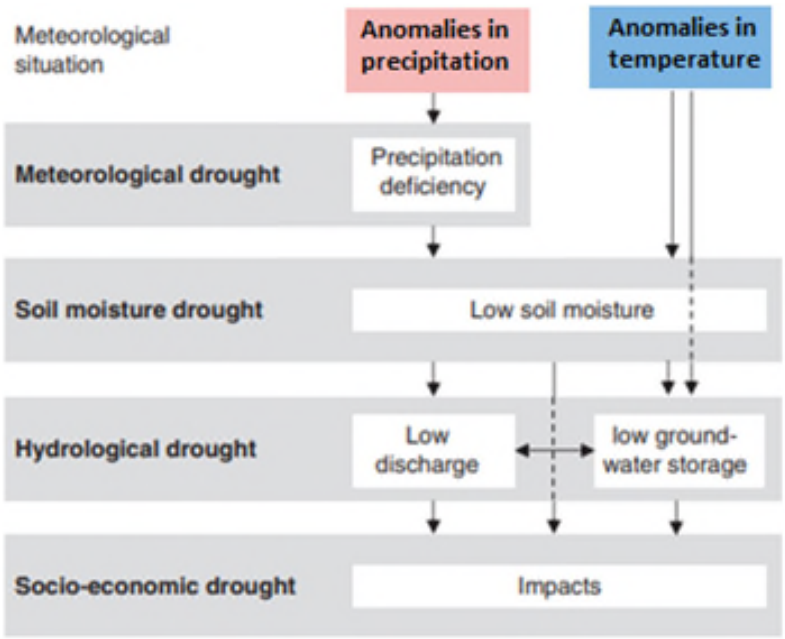

Figure 1. The direct causes and the progression of the four phases of drought, ultimately leading to undesired impacts (reprinted from van Loon, 2015, p. 363).

Meteorological drought is considered a natural hazard due to climatic variability; similarly, hydrological drought is conceptually separated from water stress, a situation of excessive human water demand (Van Loon & Van Lanen, 2013; Wilhite, 2005). Van Loon & Van Lanen (2013) point out the confusion between these two terms and argue the need for their distinction: one can apply mitigation measures to reduce water stress while one can only adapt to drought. While this is a valid point, the fact still remains that, for water management purposes, it is difficult to separate the natural hazard of drought from the human-induced water stress. At this day and age, the hydrological cycle is significantly interconnected with human activities (Yoshihide Wada et al., 2017). This is even more the case when one considers climate change due to increased greenhouse gas emissions having an effect on meteorological drought frequency and severity. This ultimately leads to changes in hydrological drought patterns (Van

Huijgevoort et al., 2014; Wanders et al., 2015). In addition, studies show that droughts are intensified by human water management, especially groundwater pumping (He et al., 2017; Margariti et al., 2019; Y. Wada et al., 2011, 2013).

In order to deal with this situation in the Netherlands, where water stress is already a reality (*Aqueduct Water Risk Atlas*, 2019), managed aquifer recharge can be used as a hydrological drought prevention measure.

2.2 The use of Managed Aquifer Recharge for increasing water availability

According to an extensive literature review by Dillon et al. (2019), there are four main methods within MAR employed worldwide, especially in regions where freshwater resources are scarce. These are streambed channel modification, riverbank filtration, water spreading and recharge wells.

Streambed channel modification has been widely applied in more arid areas to enhance supply for drinking water production and irrigation (Dashora et al., 2018). This MAR method includes small structures along streams, such as dams, that retain surface runoff in order to favor infiltration into the aquifer. Next, Riverbank filtration is a method where surface water infiltration is enhanced by pumping groundwater nearby rivers. It is mostly applied in groundwater purification for drinking water production, and research centers on its potential for adaptation to climate change and water demand (Dillon et al., 2018). Thirdly, water spreading is the intentional flooding of recharge basins. Currently research is conducted to study treated wastewater as a source for this method (Dillon et al., 2018). Lastly, recharge wells are used in aquifer storage and recovery (ASR) systems (Dillon et al., 2018).

In the Netherlands the use of riverbank filtration, spreading methods in dune filtration and ASR are used for drinking water production, with a growing use for irrigation (Stefan & Ansems, 2018). ASR is also intensively researched for thermal energy storage (Fleuchaus et al., 2018) and for freshwater lens forming in coastal aquifers to prevent saltwater abstraction (Sprenger et al., 2017). Other examples of successful pilot studies of recharge well-type measures are the Freshmaker technique (Zuurbier et al., 2015) and the controlled artificial recharge and drainage system (Pauw et al., 2015) applied at small scales in the western part of the Netherlands.

MAR systems have also recently been studied as a measure to cope with hydrological drought. One study found that MAR systems in combination with surface water abstraction have reversed groundwater depletion trends locally both in California and Arizona, increasing these areas' resilience to drought (Scanlon et al., 2016). Another study found that MAR systems have partially alleviated hydrological drought and groundwater depletion in some regions of Southern California during the past years, and that local change in recharge patterns may increase drought resilience (Wendt et al., 2018). Based on these findings it is expected that MAR will have a positive effect on hydrological drought alleviation in the Pleistocene Uplands, possibly preventing it all together.

2.3 Modeling as an approach for experimental research on hydrological drought

Using models to investigate droughts is useful in areas where there is a dense observational network of meteorological and hydrological data, such as the Netherlands. Modeling allows for a relatively simple way to explore scenarios and understand how an area responds to different treatments. Types of models used for studying hydrological drought include large scale and catchment models. Examples of large scale models are Land-surface models (LSMs), in the climatology field, and global hydrological models (GHMs), in the hydrology field (Haddeland et al., 2011). GHMs, because of their global scale, are conceptual spatially distributed models which calculate the water balance of catchments at 0.1^0 to 1.0^0 resolution.

When studying drought at finer spatial resolutions typically catchment models are used that quantify hydrological fluxes in scale <0.1. These models simulates rainfall-runoff processes and have mainly been used to research causes and impacts of drought in a region. Examples of models used include HBV (Vasiliades et al., 2017), and SWAT (Valiya Veettil & Mishra, 2020), all of which are semi-distributed and conceptual models. These types of models are more focused on runoff and streamflow, often with simple groundwater modules to account for baseflow. This makes it more difficult to apply them to study the subsurface dynamics with MAR techniques. A fully integrated surface-groundwater model which is spatially distributed and has been used for this purpose is MIKE SHE (Mauck et al., 2017). Mauck (2017) aimed at identifying potential opportunities of MAR for sustainable water management in Cape Town. Another study (Göbel et al., 2004) researched the effects of MAR using storm water on restoring groundwater levels with the GwNEU, HYDRUS 2D and SPRING models in Germany. GwNEU and HYDRUS 2D were used to quantify the natural recharge and storm water infiltration due to MAR, respectively, which were used as inputs for SPRING to simulate groundwater levels. Mooers et al. (2018) made a similar study by coupling the hydrologic model PCSWMM and the groundwater model MODFLOW to understand the effect of storm water infiltration on aquifer recharge in an urban area in Canada.

Considering the wide array of models presented above, MODFLOW is the most widely used model in MAR studies (Ringleb et al., 2016). For this thesis iMOD, an adapted version of MODFLOW developed by the research institute Deltares, was chosen. It carries all the advantages of the well-documented, open source and widely used model that is MODFLOW (Harbaugh, 2005) and allows for fast high-resolution modeling and easy geographical and 3D visualization (Vermeulen et al., 2019), important elements when checking the progress of the modeling process. Like its parent, MODFLOW, iMOD is a spatially distributed model that uses the finite-difference approach to calculate water balance with Darcy's Law and allows for 2D and 3D groundwater models. Another advantage is its coupling to MetaSWAP, a version of SWAP, which models the soil-water-atmosphere-plant hydrological continuum at a large scale (Van Walsum & Veldhuizen, 2011). The combination of MODFLOW and MetaSWAP in iMOD make this an appropriate model for this research.

3. Materials and methods

3.1 Description of the Pleistocene uplands

The Pleistocene uplands are a geological landscape located to the North, Mid-east and South of the Netherlands (Figure 2). Its name is attributed to the Pleistocene Epoch, during which the landscape was formed (Kasse, 1997; Wesselingh, n.d.). Although characterized as sandy grounds, the Pleistocene uplands vary according to location.

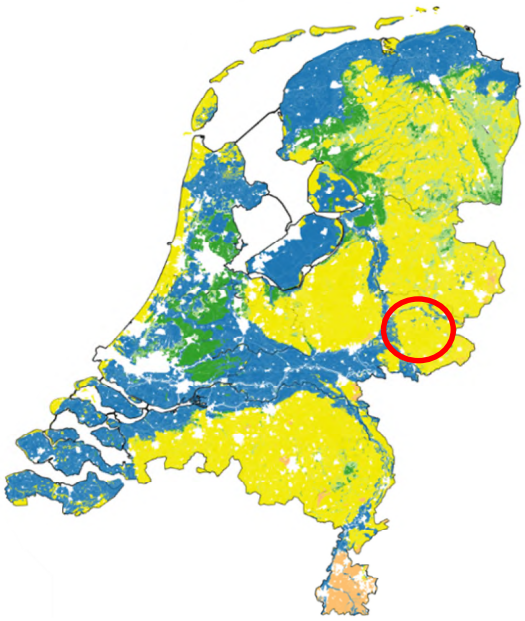

Figure 2. Map of the Netherlands and the major soil classes found in the country, according to Wösten et al. (2013) (Reprinted from Kroes et al., 2018, p. 2943). The colors represent: dark green is peat, light green is peat moor, blue is clay, peach-orange is loam and yellow is sand. The sandy areas to the North, East and South represent the Pleistocene uplands. The area circled in red is the Achterhoek region on which the hypothetical model of this thesis is based.

The general hydrogeological characteristics of the region consist of a conductive surface and highly conductive subsurface with the presence of clay lenses acting as aquitards. These characteristics make the uplands in general highly susceptible to seasonal precipitation variations (Jalink & van Doorn, 2017), since the water that infiltrates and recharges the groundwater quickly drains through the soil. Residence times in the subsurface are reduced even more by anthropogenic drainage practices in agricultural and urban areas (Jalink & van Doorn, 2017; Sterk & Wamelink, 2019).

Jalink and van Doorn (2017) report that in the areas of the cover sands, the most common landscape of the Pleistocene uplands, recharge areas are located in the sand ridges. Here groundwater levels are deeper, flowing to seepage faces in stream valleys. Because the recharge areas are less fertile, they tend to be reserved for natural vegetation with little dependence on water, such as dry heather, reforested coniferous woods and older deciduous forests. On the other hand, the depressions near brooks are used for agriculture (Jalink & van Doorn, 2017). According to the report, on average, groundwater levels in the headwater of these areas are dynamic, because they are strongly dependent on precipitation variation; when taking a regional scale perspective, however, less dynamism can be seen.

In the Veluwe, groundwater levels are much deeper, making it suitable for the same type of vegetation found on the sand ridges and unsuitable for agriculture (Jalink & van Doorn, 2017). Because of the large elevation difference between the top of the moraine and its base, as well as the tilted clay layers in the moraine, groundwater head gradients are present in a highly stable groundwater system, generating permanent seepage faces that react in the order of 2 to 3 years to variations in precipitation (Jalink & van Doorn, 2017; Verhagen et al., 2014). Near these seepage faces and the streams they feed, water-dependent nature used to be present, but they currently have been transformed into agricultural or urban areas that undergo intense drainage (Jalink & van Doorn, 2017).

3.2 Conceptual Model

The Achterhoek region (circled in red in Figure 2) was chosen as a type of blueprint for the thesis model because it fits the description of a typical cover sand landscape. Looking at its lithology and geohydrological characteristics, the Achterhoek region provides the basis for a hypothetical model which

can represent the standard situation of what could happen to the groundwater systems of the Pleistocene uplands when MAR is applied. Its lithological profile includes a relatively thin and highly permeable soil layer above a thick clay layer that dips in the direction of groundwater flow. This fairly simple-to-be modeled hydrogeological situation resembles the schematic vertical cross-section of the Pleistocene uplands seen in Figure 3.

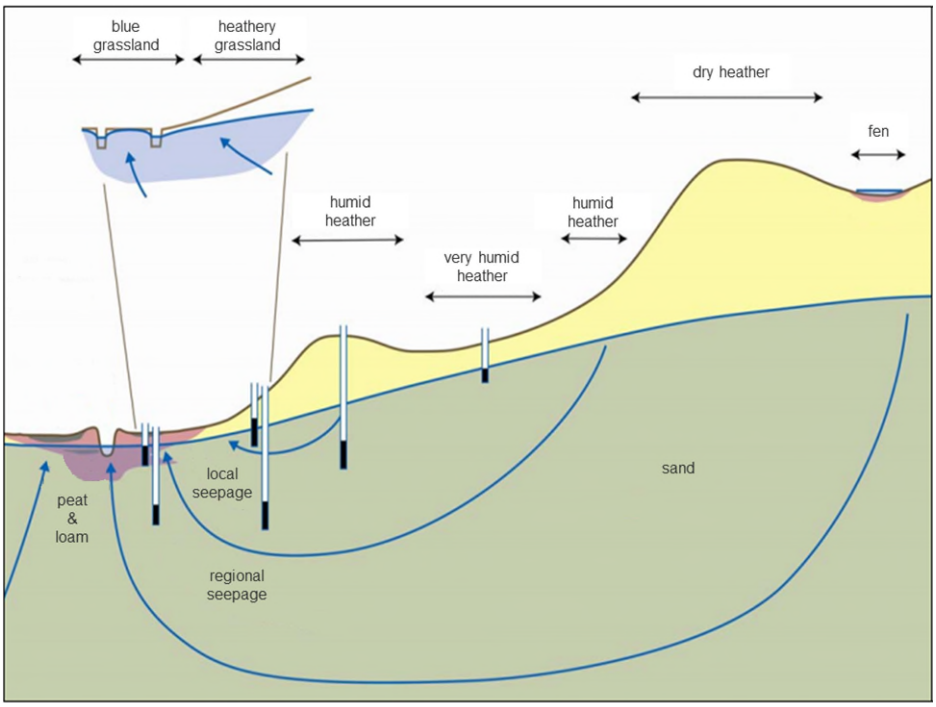

Figure 3. Schematic vertical cross section of the Pleistocene uplands, the natural vegetation types present and the direction of groundwater flow (translated from Witte et al., 2007, p. 78). The schematization is at a regional scale and is used as a layout for the hypothetical study area and the building of the model.

The hypothetical model spans a region of 15 km long and 15 km wide. The average hill slope is 0.001 in the east-west direction. The whole width of the model at the downhill area (the western boundary) is delimited by a river for which the characteristics were taken from the IJssel River. Reflecting the scheme in Figure 3 rather than the land use practices described for the cover sand areas, the vegetation follows the hill slope: wetland downhill in the floodplain of the river, natural grassland as a transition zone where seepage faces are present and agricultural grassland uphill.

The 13 scenarios in the modeling experiment represent different strategies in applying an injection well field as the MAR measure. The first is a baseline simulation with no MAR, representing the "do nothing" strategy. This is used in the modeling experiment in order to observe the effects of hydrological drought and to derive drought threshold values of groundwater levels. A batch of 6 scenarios consists of applying MAR near the western border at the agricultural land use area, and are named AG MAR. The other batch of 6 MAR scenarios have the same characteristics as the previous batch, but are located at the eastern border, between the wetland and natural grassland. This batch is named N MAR. In each batch water is injected during the winter for 3 scenarios, rendering the idea of infiltrating a part of the abundant surface water from rivers during this season. In the remaining 3 scenarios water is infiltrated during the summer, where the source of water could be treated effluent or surface water. Both the winter and summer treatments have the same varying recharge quantities per well: 500 m^3/d, 5000 m^3/d and 10000 m^3/d. A summary of the 12 MAR scenarios can be seen in Figure 4.

The present choice of scenarios allows for a sensitivity analysis of the effects of location, season and recharge quantity on the regional extent of MAR effectiveness for alleviating the effects of drought in the Pleistocene uplands. The baseline scenario spans 30 years, from January 1990 to December 2019, while the MAR scenarios span 10 years from January 2010 to December 2019.

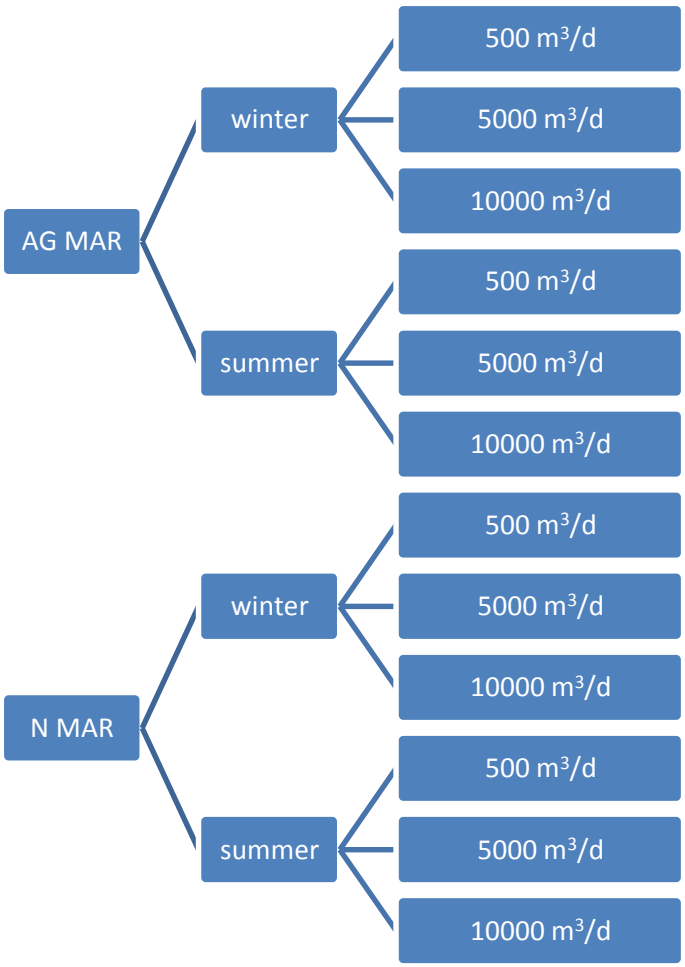

Figure 4. Tree diagram of all MAR scenarios applied in this thesis.

3.3 Model setup

The 3D hypothetical model of the Dutch Pleistocene uplands was built in iMOD version 5.0 (Deltares, 2019). In order to have a more realistic basis, the vertical model geometry was based on a simplified cross section of the subsurface model BRO Regis II v2.2 in DINOloket given by 5 boreholes: B41A0105 at Halle Heide, B34C0041, B34C0112, B34C0056 and B34A0098 at the Berkel river between Zutphen and Lochem in the Gelderland Province (TNO, 2017). The total depth of the soil profile was 126m considering the highest point of the surface level and the lowest point of the last layer.

The model cell size was set to 250 by 250 m and the layers consisted of 3 layers of aquifers and an aquitard between layers 2 and 3. The hydrological base corresponded to a thick clay layer of the Breda formation. The first layer was based on a sandy unit of the Boxtel formation, the second on a sandy unit of the Kreftenheye formation, and the third on a sandy unit of the Oosterhout formation. The aquitard corresponded to a clayey unit of the Oosterhout formation. Layers 1 and 2 were modeled as one unconfined aquifer and layer 3 as a confined aquifer. The profile of the layers can be seen in Figure 5.

The model's horizontal geometry was based, but modified for simplicity, on the *Actueel Hoogtebestand Nederland 1* (AHN1) 25 m resolution map in the PDOK viewer (2012) for the surface level topography. The map's northwest and southeast x and y coordinates were (205000, 465000) and (220000, 450000) respectively. The surface level topography can be seen in Figure 6.

The hydrogeological characteristics of horizontal and vertical conductivities were based on the BRO REGIS subsurface model (TNO, 2017) for each of the layers, except layer 3, which was changed

during model calibration. The hydraulic conductivities used were 6.25, 75 and 40 m/d for the horizontal conductivities of layers 1, 2 and 3, respectively and 0.0035 m/d for the vertical conductivity of the semi-confining bed below layer 2. Anisotropy was set to 1. Since the iMODFLOW version used for this thesis does not support the option of modeling unconfined aquifers directly, specific yields were adopted as storage coefficients to force the top two layers of the model to behave like so, as suggested by the user manual (Vermeulen et al., 2019). A specific yield of 0.24 was used for the for the first two layers, while for the third layer the storage coefficient was calculated as a product of the layer thickness and the specific storage of $1.0x10^{-5}$ m^{-1}.

A transient time discretization of 10957 stress periods (one for every day) was applied to the baseline and MAR scenarios of the model. There were seasonal changes, described below, applied on the stress periods marking each April 01, the beginning of the summer, and October 10, the beginning of the winter. The years used for the simulations were 1990 to 2019 for all scenarios, which were run for 30 years in order to guarantee the same initial conditions at the beginning of 2010, the year MAR was introduced.

The river package was used to place a river on the western border of the first and second layers, while the western border of the third layer was set to constant head. All other borders where set to no-flow boundary conditions. The bottom elevation values of the river were set to 1.0 m above the Amsterdam Ordnance Datum (NAP) and the conductance to 75 m/d. The conductance was applied to the whole area of the cell and a riverbed thickness of 0.5m, totaling a value of $9.375x10^{7}$ m^2/d . The stage varied with the stress period: 6.0 m and 4.8 m above NAP for winter and summer, respectively in order to simulate the high winter and low summer river discharges.

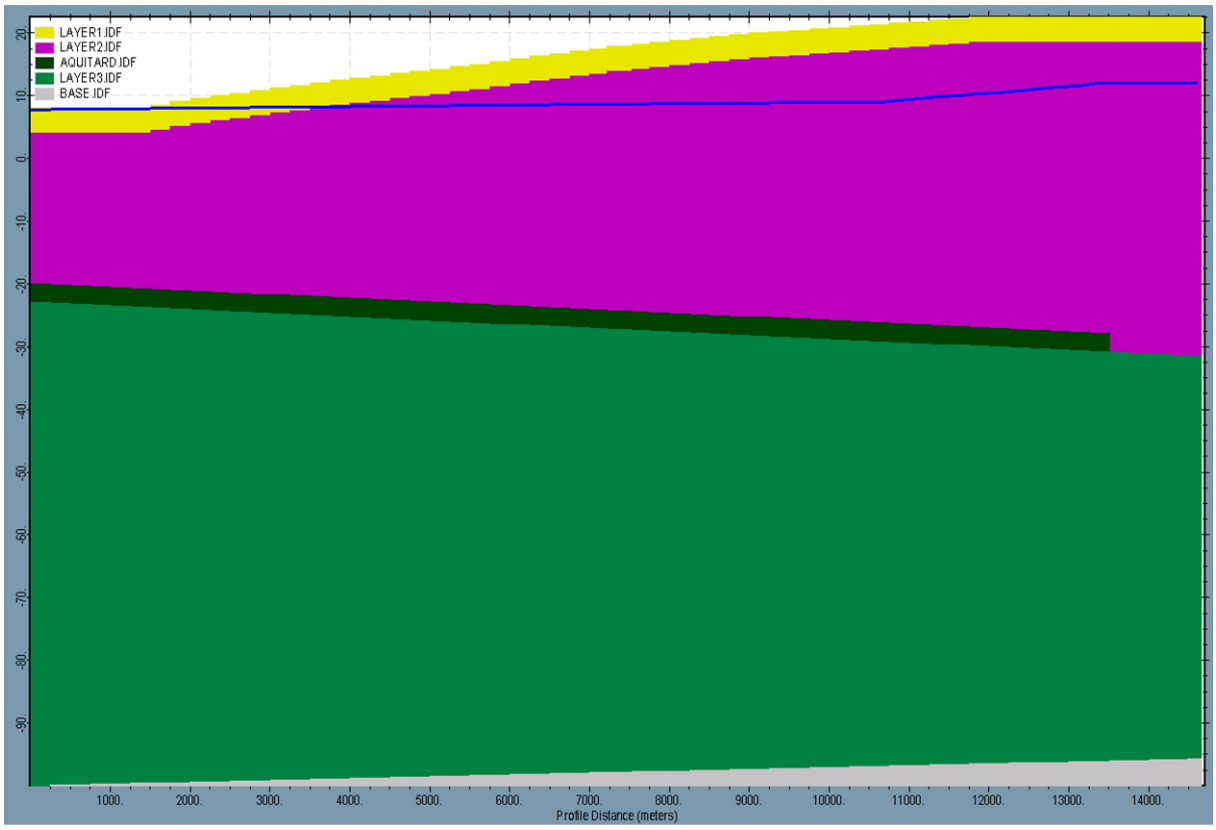

Figure 5. Model layer cross section from east (x = 0) to west (x = 15000 m) and from 26 m above the Amsterdam Ordnance Datum (NAP) (z = 25 m) to 100 m below NAP (z = -100 m). The dark blue line corresponds to the initial level of the groundwater table. The layer numbering is as follows: layer 1 in yellow is a sandy unit of the Boxtel formation, layer 2 in purple is a sandy unit of the Kreftenheye formation, the aquitard in dark green is a clayey layer of the Oosterhout formation, layer 3 in blue green is a sandy unit

of the Oosterhout formation, and in gray is the hydrological base corresponding to the thick clay layer of the Breda formation. Note that the aquitard is not consistent across the region. This is to simulate the presence of clay lenses common to the Pleistocene uplands.

The well package was used for modeling the MAR system. To model recharge of the aquifer, a well field of 11 wells was placed along a line spanning from north to south at a distance of 1 to 1.5 km from each other and between 2 to 2.5 km from the western (N MAR) or eastern border (AG MAR) of the model (Figure 6). For the winter MAR scenarios, wells were turned on for the winter stress periods and off during the summer stress periods from 2010 to 2019. The opposite was done for the summer MAR scenarios. Table 1 shows the recharge rates and total yearly volumes applied. The well screens were made to be 1 meter in height, ranging from a depth of 0 to -1 m NAP, in layer 2. Besides the injection wells, a series of 12 observation wells were placed in the model so as to collect time series results. Their distribution can be seen in Figure 6.

Table 1. Approximate total well field recharge rates in different units of the varying MAR scenarios. The rates in mm were calculated based on the active model area (without the inactive no-flow boundary and river cells) of 2.10×10^8 m^2. For comparison: the IJssel River's average discharge in the year of 2018 was 419 m^3/s at Deventer (Rijkswaterstaat, 2020).

Well recharge rate	Total well field recharge rate			Actual yearly recharge volumes (6 months)	
(m^3/d)	(m^3/s)	(m^3/d)	(mm/d)	m^3	mm
500	0.0636	5500	0.0262	0.99×10^6	4.55
5000	0.636	55000	0.262	9.9×10^6	45.5
10000	1.27	110000	0.524	19.8×10^6	90.9

In order to obtain the initial groundwater heads, firstly a steady state model was run with winter river stages, no MAR wells and constant recharge of 0.767 mm/d. The initial heads from the unconfined aquifer were calculated from the top surface of the first layer based on an average hydraulic gradient of 0.0003 m/m from east to west of the model (Figure 5). The initial hydraulic heads of the confined aquifer were set to be 5 meters less than those of the unconfined aquifer. The resulting groundwater heads of the steady state model were used as the starting heads for all scenarios.

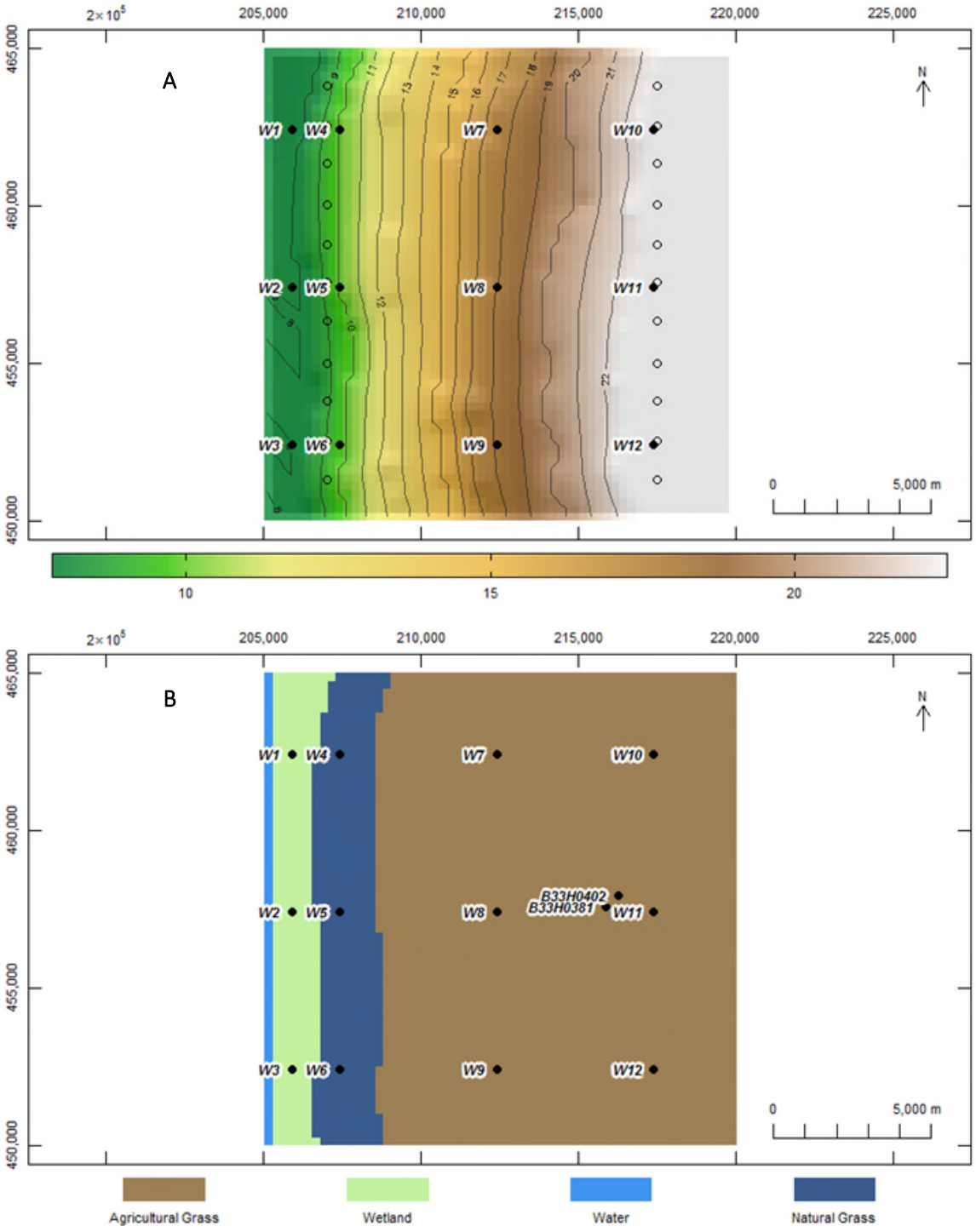

Figure 6. Top view of the model's land surface topography (A) and land use (B). The unfilled dots in plot A show the position of the 11 injection wells in the AG MAR scenarios (eastern border) and the 11 injection wells in the N MAR scenario (western border). Plots A and B show the 12 model observation wells (the filled dots W1 to W12), and plot B also displays the two observation wells (B33H0402 and B33H0381) from the DINOloket groundwater database.

The MetaSWAP module, version 8.0.0.7 (Van Walsum et al., 2019) was used to model the unsaturated zone, the soil – plant – atmosphere interactions, and to couple these to the first layer of the groundwater model in iMOD. From this package the model received its transient atmospheric boundary conditions. The model used daily precipitation and evaporation time series data from the KNMI weather station in Deelen (2019b) from 1990 to 2019.

The soil type applied was a weak loamy sandy soil with coarse sand underneath, which corresponds to soil number 305 in the National Hydrological Model (LHM) soil database (Wösten et al., 2013). Land use was applied to the model based on the soil surface elevation. Elevations greater than 13.5 m above NAP had agricultural grass, between 13.5 and 8.5m had natural grass, and elevations below 8.5 m had natural wetlands (Figure 6). No irrigation was applied to the agricultural grass in order to understand the full extent of the drought effects. Drought stress parameters were applied based on values used for other drought research at KWR. Oxygen stress was disabled because it was found that the code of the current version of MetaSWAP still has inconsistencies regarding this parameter. A summary of the model input parameters for both the baseline and the MAR scenarios can be seen in Table 2.

Table 2. Summary of the model input parameters and descriptions per layer and package used. Elevation is based on the Amsterdam Ordnance Datum (NAP).

iMOD Package	Data Set	Layers	Description
Boundary conditions	BND	1 & 2	Head-dependent flux boundary using RIV package (Western border). No-flow (North, South & Eastern borders).
		3	Constant head boundary at the Western border. No-flow (North, South & Eastern borders).
Surface elevation & Soil profile	TOP	1	Elevation ranges from 25m to 7.8 m. Based on the AHN1 data set.
	TOP & BOT	1-3	Total thickness ranges from 65 to 107 m. Based on the BRO Regis II subsurface model of the Achterhoek region.
Horizontal conductivity	KHV	1	6.25 m/d
		2	75 m/d
		3	40 m/d
Horizontal – vertical anisotropy	KVA	1-3	1.0
Vertical conductivity	KVV	1	11.54 m/d
		2	0.0035 m/d (semi-confining bed below Layer 2)
Initial heads	SHD	1 & 2	*Steady state:* Follows the surface level topography with an average hydraulic gradient of 3.0×10^{-4} from East to West. *Baseline & MAR*: resulting steady state heads.
		3	*Steady state*: 5 m less than the initial heads for 1 &2. *Baseline & MAR*: resulting steady state heads.
Confined storage coefficient	STO	1&2	0.24
		3	1.0×10^{-5} m^{-1} * thickness of layer 3
Head-dependent flux boundary (river)	RIV	1 &2	Conductance = 9.375×10^{7} m^2/d Bottom elevation = 1.0 m River stage winter = 6.0 m River stage summer = 4.8 m Infiltration factor = 1.0

Injection wells	WEL	2	Top screen elevation = 0 m Bottom screen elevation = -1 m
			Number of injection wells = 11 (locations differ according to scenario)
			Injected discharge per well = 500, 5000 and 10000 m^3/d (depending on scenario)
MetaSWAP (CAP)	Atmospheric boundary	1	Precipitation and evapotranspiration time series data between 01/01/1990 – 31/12/2019 from KNMI (2019b).
	Soil type		305 (fine, weak loamy sand above a coarse sand layer) (Wösten et al., 2013)
	Land use		Elevation > 13.5m: agricultural grass with irrigation 13.5m ≥ elevation ≥ 8.5m: natural grass 8.5 m > elevation: natural wetlands
	Feddes function threshold parameters for oxygen and drought stress		High potential evapotranspiration (PET) rate = 5 mm/d Low PET rate = 1 mm/d *Pressure heads (m) [wetland; natural grass; agricultural grass]:* Oxygen stress = disabled; disabled; disabled Optimal water uptake = -0.01; -0.01; -0.25 Suboptimal water uptake (high PET) = -2; -2; -2 Suboptimal water uptake (low PET) = -8; -8; -8 Drought stress = -80; -80; -80
	Soil hydraulic parameters	1	Maximum allowed ponding depth = up to 0.5 m in the wetland area. Runoff Resistance = 1 d Runon Resistance = 1 d Infiltration Capacity = 5 m/d Soil Moisture Factor = 1 Soil Permeability Factor = 1

3.4 Model analysis methods

Before the different transient scenarios were applied, the steady state model was calibrated against realistic theoretical groundwater levels. The parameters for the steady state model were changed until the spatial distribution of groundwater heads followed the trends seen in Figure 3.

In order to validate the model, the baseline scenario was compared with observed groundwater levels. Groundwater level time series were downloaded from DINOloket (TNO, 2019) from 9 observation wells located in the region corresponding to the hypothetical model. Since the nine wells show the same groundwater fluctuation patterns, only two were chosen (B33H0381 and B33H0402) as a reference for comparison with the model data. The time series used was from 14/01/2010 to 28/12/2019. The groundwater levels of both the model and the observations were divided by their respective time series mean value in order to have them normalized and make them more comparable.

Next, the baseline scenario time series of each observation well was analyzed for patterns in groundwater fluctuation. A margin of three years (01/01/1990 to 31/12/1992) from the begin from the model was used as a period for model spin up. Mean groundwater levels were calculated considering the entire 30 years and another set of mean levels were calculated based on only the 27 years after the allocated spin up period. The same process was done for the drought threshold levels. The 30 year mean and threshold were compared to the 27 year mean and threshold, respectively, in order to decide whether to discard the spin up period in the analysis. It was found that there was little difference between the values when using the entire or the shorter period (see Appendix A), therefore the entire 30 year time series was used to calculate the threshold.

In theory model spin up could take much longer than the amount of time simulated, in which case considering only three years of spin up time would not show a difference. Although this may be the case, it is important that the drought threshold be calculated based on a consistent time series without differences due to spin up influence within it. This was the case in the time series of the baseline simulation, from which the thresholds were obtained.

Drought thresholds were calculated for each observation well in order to characterize hydrological drought. The fixed threshold method (Sarailidis et al., 2019) was chosen for this thesis, and was established to be the groundwater level that exceeded 80% of the time. Periods of the time series where groundwater levels fell below this threshold were considered to be periods of hydrological drought.

The time series results of evapotranspiration, infiltration, groundwater recharge and level of the baseline scenario were observed to pinpoint the occurrence of drought and understand the dynamics of the model. In order to determine the regional effects of MAR for drought prevention, the groundwater level time series from 2010 to 2019 of the 12 observation wells from all scenarios were compared to each other with regard to the drought threshold. In addition, the time series of the relative transpiration (the ratio between the actual and the potential transpirations) at the location of the observation wells were compared. The comparisons of the relative transpiration were characterized in terms of magnitude in order to understand which scenarios were more effective in increasing transpiration.

4. Results

4.1 Steady state model

In the steady state model, groundwater heads of the unconfined aquifer, formed by layers 1 and 2 (Figure 7), follow typical spatial patterns of groundwater levels along a hill slope in the Pleistocene uplands (Jalink & van Doorn, 2017; A. van Loon et al., 2014). Levels are deeper uphill, reaching depths below 2 m. At a distance between 2 and 6 km away from the river, groundwater is at or above the surface, making this area a seepage zone. Within 1 km from the river, groundwater levels are between 1 to 2 m deep.

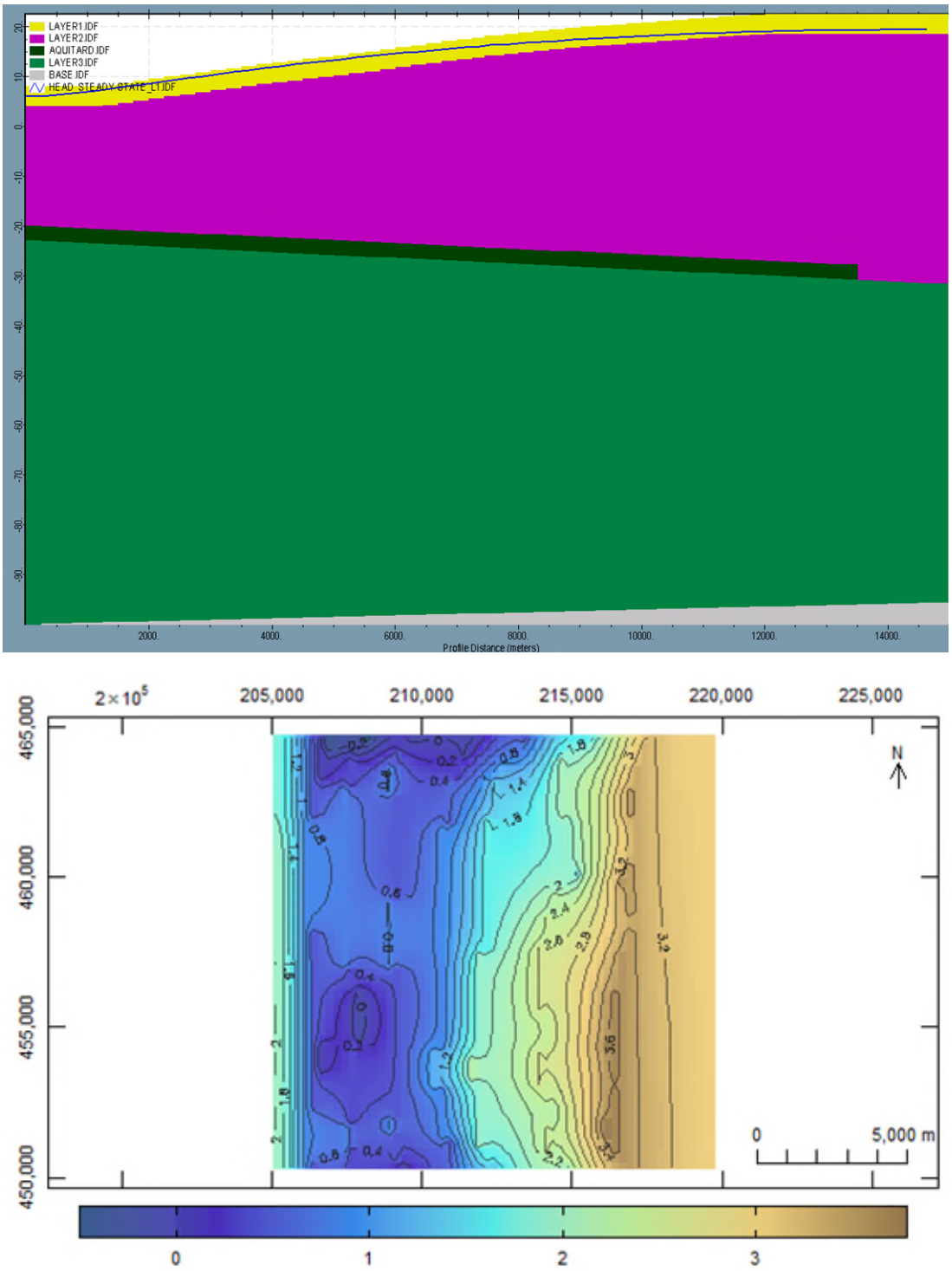

Figure 7. At the top: Vertical cross section of the model from east (x = 0) to west (x = 15000 m) and from 26 m above the Amsterdam Ordnance Datum (NAP) (z = 25 m) to 100 m below NAP (z = -100 m). The dark blue line corresponds to the groundwater level reached after a steady state simulation considering winter conditions for the river stages. At the bottom: Top view of the spatial distribution of the groundwater depths after a steady state simulation considering winter conditions for the river stages.

When running the steady state model, it was discovered how sensitive the groundwater heads are to the hydraulic conductivity of the third layer. This third layer represents the regional groundwater system which flows underneath a very resistant aquitard. It was expected that there would be less influence from this system on the unconfined aquifer above it, but instead they are closely connected. A probable reason for this the "hole" in the aquitard at the model's western border. The original value of saturated hydraulic conductivity of the third layer, which was based DINOloket data (TNO, 2017), had to

be increased from 7.5 m/d to 40 m/d after model calibration. Even though the former value corresponds to realistic conditions in the Achterhoek region, it was not possible to use it without resulting in grossly overestimated groundwater heads for the unconfined aquifer. A reason for this large difference is the model's lack of local drainage systems. In reality the region is filled with smaller rivers feeding the IJssel, little channels and drains, all of which are not present in the hypothetical model. Increasing the conductivity parameter of the third layer decreased the head gradient of the top two layers, making up for the lack of drainage systems.

In addition, a constant head boundary value of 5 meters below the starting heads of the first two layers was applied to layer 3 in order to minimize its influence on the top two. This was found to be an approximately optimal value: decreasing it had little effect on the drainage capacity of the third layer, which was much more influence by hydraulic conductivity; increasing it caused water to flow in from the constant head boundary instead of leaving through it.

4.2 Baseline scenario

4.2.1 Groundwater

Model validation

Comparing the DINOloket measured groundwater data at wells B33H0381 and B33H0402 with the model observation wells (Figure 8), it is possible to see that both measured and simulated data display similar trends but different fluctuation patterns. The measured data show much more regularity in the fluctuation, which is not entirely the case with the simulated data. At the wetland observation wells fluctuations are more similar. The farther away from the western border and the river, the more difference in fluctuation between measured and simulated groundwater level patterns. This behavior is attributed to the lack of drainage and other river systems in the model in comparison to the Achterhoek.

The model responds more intensely to atmospheric conditions, especially at the higher elevations, accumulating more water in wet years such as 2015 and 2016, and losing more water in dry years such as the summer droughts of 2018 and 2019. The greater capacity to store water in wetter years shows the potential these locations have in accumulating more water in the model subsurface. On the other hand, if a year has a lower average precipitation, groundwater levels may become quite low. This is the case in the second half of 2013, where groundwater levels in the natural and agricultural grasslands show a low dip. One can see from the low precipitation during the first half of the year (see Appendix B) that groundwater levels react intensely to it. This is important to note, because such a dip in groundwater levels is seen in the measured data. In fact, the period of low precipitation in 2013 are in between periods of intense and high precipitation. The reality shows that the groundwater system had a larger buffer to cope with such a situation compared to the model.

Another difference is the model's response time. With increasing distance from the river, groundwater levels at the model observation wells display a slight lag in fluctuation compared to those measured. This has to do with the increase in reaction time between meteorological conditions and groundwater levels in areas with thicker unsaturated zones, such as the Veluwe (Verhagen et al., 2014).

Nevertheless, in both data sets the summer droughts of 2018 and 2019 can be seen, especially at the natural and agricultural grassland wells. The period length of low groundwater levels are similar, as well as the relative magnitude of their decrease. This is an indication that the hypothetical model successfully represents the dynamics of the general groundwater system.

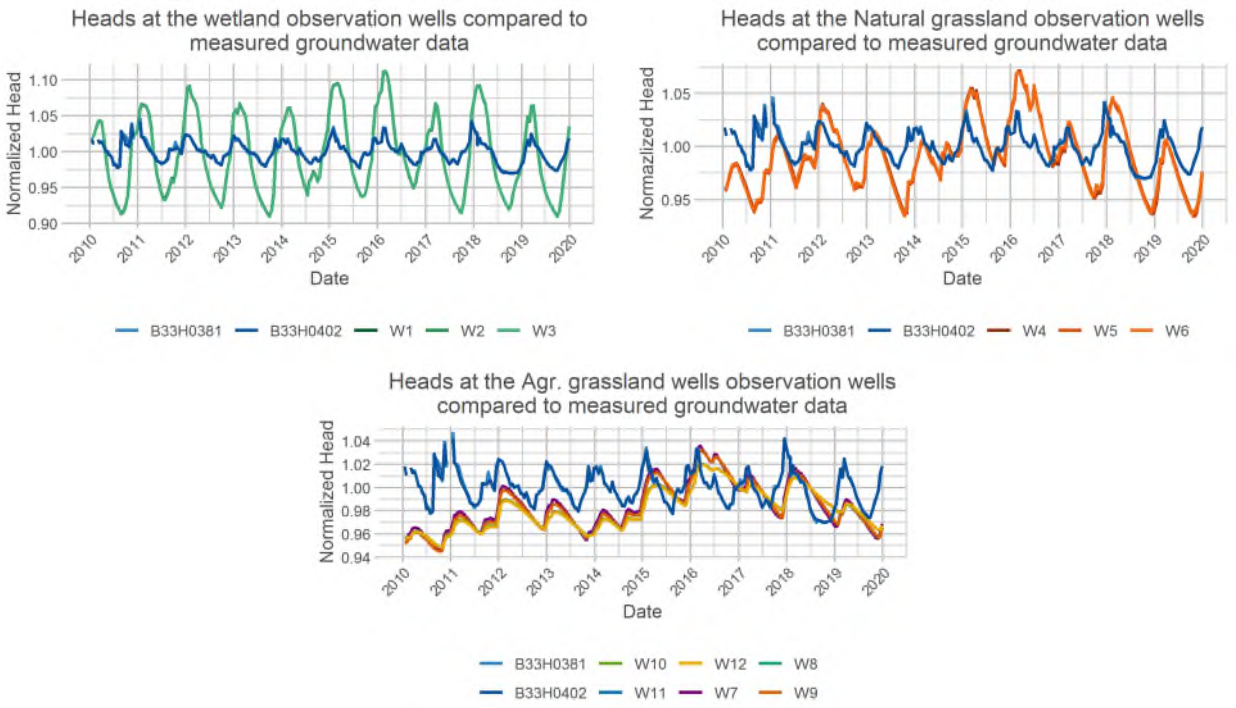

Figure 8. Comparison between the groundwater levels at two wells from the DINOloket database (B33H0381 and B33H0402) and the heads calculated in the baseline scenario model run at the 12 observation wells distributed in the wetland (top left), natural grass (top right) and agricultural grass (bottom) land use areas.

Groundwater Results

As discussed in the previous section, the groundwater levels varied according to elevation and distance from the river. For this reason the time series of four observation wells are shown below in Figure 9. An overview of all wells is to be seen in Appendix B.

At well 2, located in the wetland area and closest to the river, groundwater levels are frequently within a meter from the surface level and the drought threshold is a little less than 2 m below the surface. Because groundwater has a more uniform fluctuation pattern, extreme wet or dry years are more difficult to distinguish from one another. It seems that almost all years suffer a drought, yet every time levels are fully recovered. This is due to the influence of the seasonal river stage changes implemented in the model. Since river levels have a meter difference between winter and summer, the groundwater heads in its vicinity fluctuate accordingly. In addition, contrarily to what is seen at the wells at the higher elevations, there is no groundwater mounding close to the river, which drains the excess water away.

At well 5, in the natural grassland area, groundwater levels are occasionally within 50 cm of the surface, since the location is a seepage zone, but also easily fall below the drought threshold. A high frequency of sharp changes still occurs, although less uniformly than at well 2. Here the influence of the river is still present but less determining, and differences between wet and dry periods are more visible.

Wells 8 and 11, all within the agricultural grassland, are located at different elevation levels (Figure 6). At well 8 groundwater levels on average seem to be around 2 to 3 m below the surface level, while at well 11 they are between 3 and 4 m below the surface. These wells show a clear distinction between wet and dry periods caused by meteorological conditions, since there is little influence from the river in that region. Also, the amplitude of groundwater level fluctuation is greater, reaching almost 2 meters between the extremes, as opposed to 1 meter in the other two wells. Moreover, the time difference between minima and maxima is longer. At these wells a clear indication of extreme years is more clearly seen: the wetter periods occur, in descending order, in the periods of 1994-1995, 2002-

2003, 2016-2017, while the drier periods reaching or surpassing the drought threshold occur in 1993, 1998, 2006-2008, 2009-2015, 2018 and 2019.

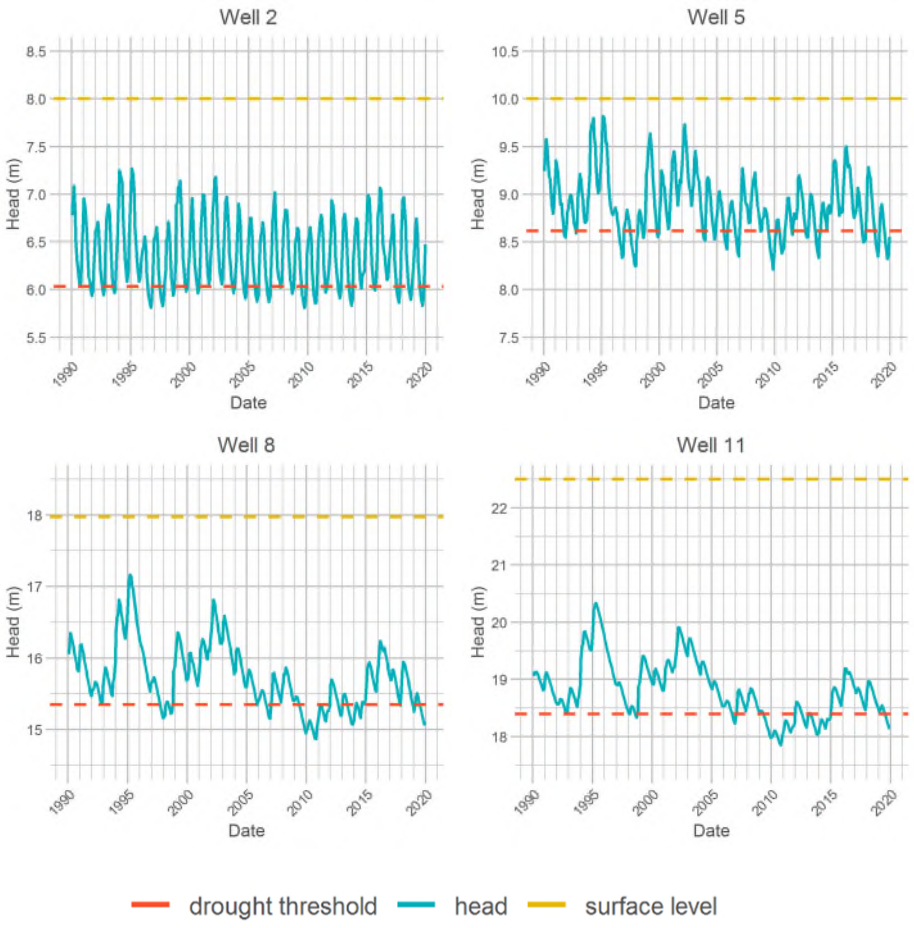

Figure 9. Groundwater heads calculated by the baseline scenario model run for 4 of the 12 observation wells. The observation wells represent a horizontal transect of the entire model domain. Heads are shown in relationship to the surface level at the well location and the drought threshold level (taken as 80% of the baseline groundwater level frequency).

Groundwater contribution to the river

The total monthly values of groundwater contribution to the river varies significantly because of the change in river level between winter and summer. The sudden increase in gradient when the river level is lowered by one meter causes sudden peaks in discharge at the beginning of the year. These sudden peaks are due to model simplifications and are not realistic, since in reality the change in river level is much more gradual. However, on the whole, the total average monthly groundwater discharge to the river is about 30.000 m^3/d, which amounts to the reasonable value of approximately 8.3 mm/d. Details can be seen in

Appendix C.

4.2.2 Unsaturated zone and vegetation

Figure 10 shows transpiration deficit in terms of relative transpiration (T_{rel}), which is the ratio between T_{act} and T_{pot}, and the soil moisture pressure heads at the root zone for well locations 2, 5, 8 and 11 in 2018 and 2019. The full 30 year time series can be seen in

Appendix E. When T_{rel} is close to one, the vegetation is close to its maximum production rate, while low T_{rel} values indicate stress of some kind. Zero value pressure heads indicates saturation, while -80 m is the wilting point for all vegetation types in the model.

Drought stress occurred in both years during summer. It was extreme in 2018, when T_{rel} decreased by almost 80% in locations 2 and 5, and more than 80% for wells 8 and 11. Pressure heads were lower than -60 m at locations 2 and 5, and almost reached the wilting point at 8 and 11. The summer of 2019 was also intensely dry as T_{rel} decreased by at least 40% at all locations and pressure heads were at about -40 m or lower.

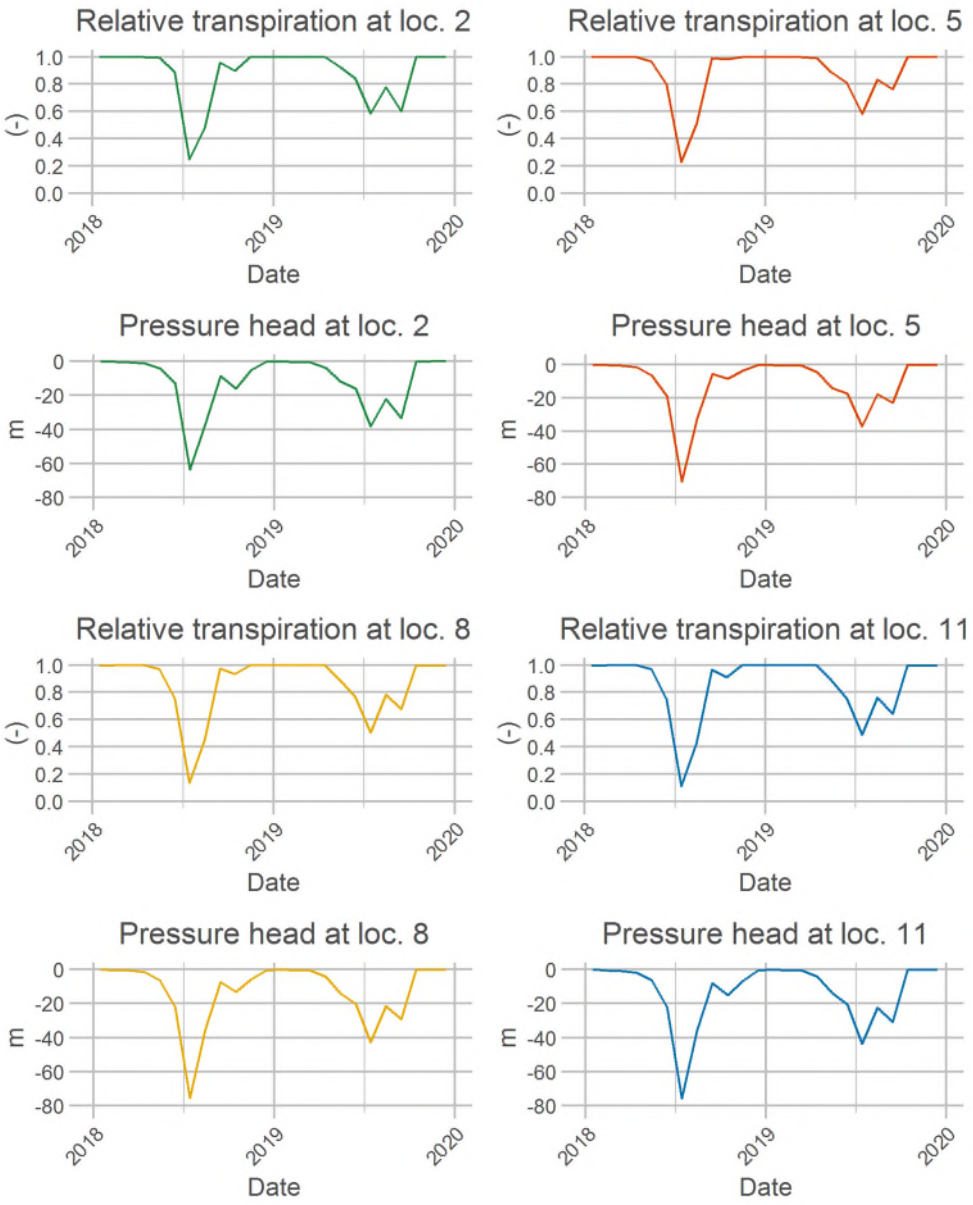

Figure 10. Mean daily values averaged over each month of the relative transpiration and pressure heads at the root zone in the vicinity of the observation wells in the wetland (location 2), natural grassland (location 5) and agricultural grassland (locations 8 and 11) areas during the three decades of the baseline simulation.

4.3 MAR scenarios

4.3.1 The regional effects of locally applied managed aquifer recharge for hydrological drought prevention

The model results show that the application of managed aquifer recharge, as proposed by this thesis, does seem to have regional success in preventing hydrological drought. In all scenarios the first five years are needed to reach the full effects of MAR. After 2015, all scenarios have reached a steady state, therefore, the analysis for the effectiveness of MAR is taken from this year on. The figures portraying the spatial distribution of the various scenarios' effects portray wells 2, 5, 8, and 11. The other time series can be seen in

Appendix G.

For the AG MAR scenarios (Figure 11), all well discharges prevent hydrological drought at well 11. Groundwater levels increase by an average of 0.25, 2.25, and 3 m for the 500, 5000 and 10000 scenarios. The summer and winter scenarios show a difference in seasonality of groundwater level increase seen by the oscillating time series, as expected, but the yearly average remains roughly the same. The winter peaks are higher and sharper since winters are periods of higher natural recharge, but the summer peaks are wider, indicating that the summer scenarios provide a buffer during the drier months. This sinusoidal behavior is mostly to be seen in scenarios 5000 and 10000, while 500 shows less difference between winter and summer.

At well 8, the 500 scenario still prevents drought up to 2018 and alleviates it in 2019 by decreasing the deficit. The 5000 and 10000 scenarios are able to prevent all drought events, and their effects are still quite significant. Groundwater level increase reaches about 0.10, 0.75 and 1.25 m in the 500, 5000 and 10000 scenarios, respectively. From this well to the other ones downhill, the difference between the summer and winter scenarios cease to show the sinusoidal behavior. At the beginning of the decade, before reaching steady states, summer scenario groundwater levels are only slightly higher than the winter scenarios, a difference which becomes imperceptible by 2015. A possible reason for this is that as groundwater flows to other regions of the groundwater system it leaves the well field's zone of influence and thus groundwater flow and levels are governed by other boundary conditions (Figure 13). For well 8 the greatest influence probably comes from the atmospheric boundary conditions.

The influence of the constant head boundary condition of the river are felt to a greater degree at wells 5 and, especially, 2. At these wells the 500 scenarios are almost insignificant, but the 5000 and 10000 scenarios are still able to alleviate drought in 2018 and 2019 since the deficits are smaller, and cause a more speedy recovery of groundwater levels above the drought threshold.

It is interesting to note that the increase of the effects with respect to the recharge amounts of the AG MAR scenarios is nonlinear. Observing the increase in groundwater levels at well 8, applying a recharge by 5000 m^3/d per well causes an increase in heads of 0.75 m from the baseline, while the up scaling from 5000 m^3/d to 10000 m^3/d causes a further increase of only 0.50. This occurs because as groundwater levels increase at the higher elevations, the groundwater head gradient increases at a higher rate. Therefore, there is an optimum as to how much water can be injected and storage increase can be seen.

In the N MAR scenarios, the spatial distribution of the effects is slightly different (Figure 12). The injection wells are located nearest well 5, where the effects of each scenario are felt the most. At this well both winter and summer applications of 5000 and 10000 are able to prevent hydrological drought in 2018 and 2019. The winter and summer applications are able to increase levels by about 0.25 and 0.50 m,

respectively. The 500 winter and summer scenarios have less significant effects, since levels are increased by a few centimeters compared to the baseline scenario, thus the drought is only slightly alleviated. Also, the 500 scenarios show insignificant effects at all other wells.

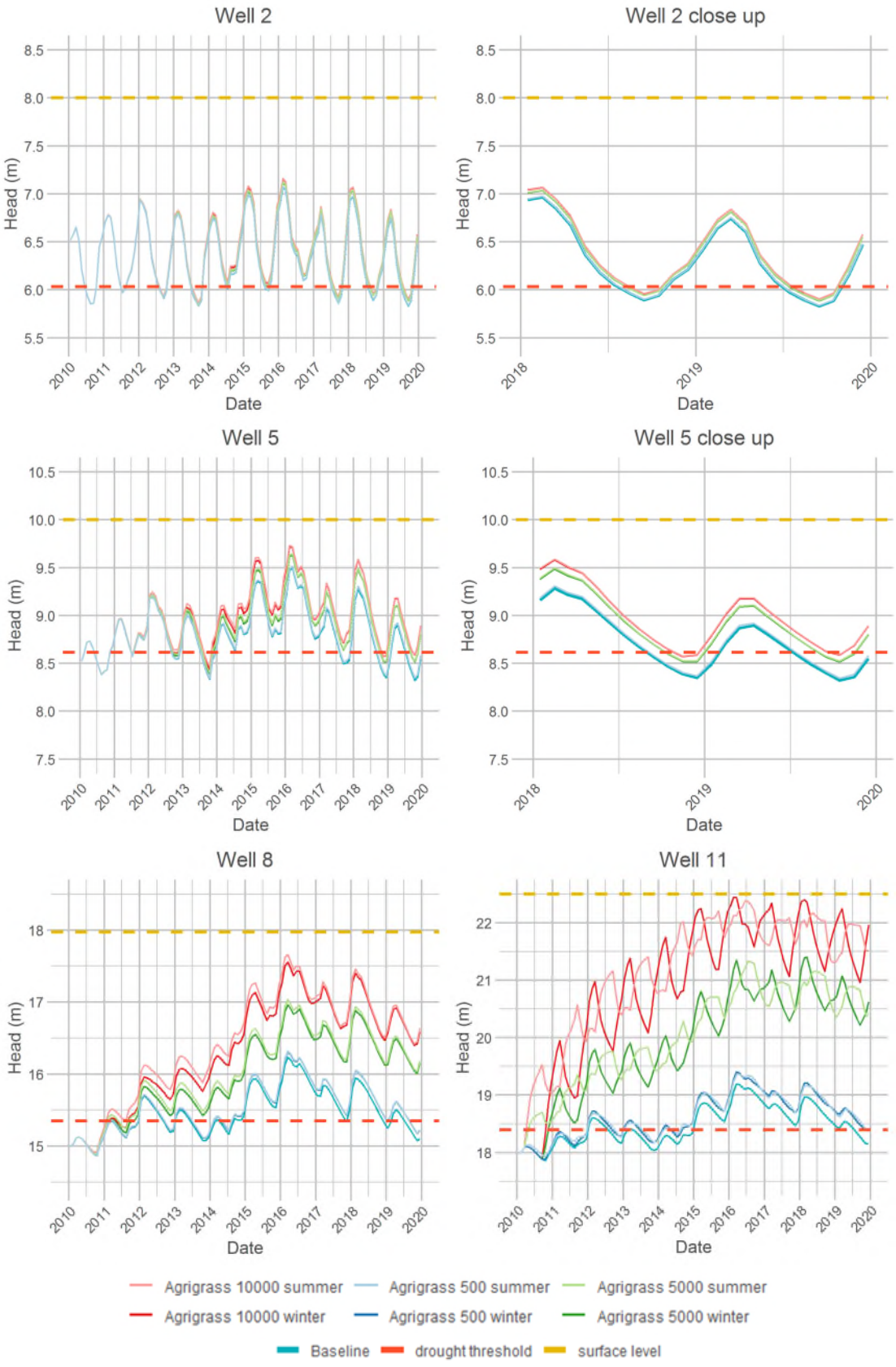

Figure 11. Comparison of the groundwater heads calculated from the baseline, MAR applied in the summer and winter in the agricultural grassland area for 4 observation wells. Heads are shown in relationship to the surface level at the well location and the drought threshold level.

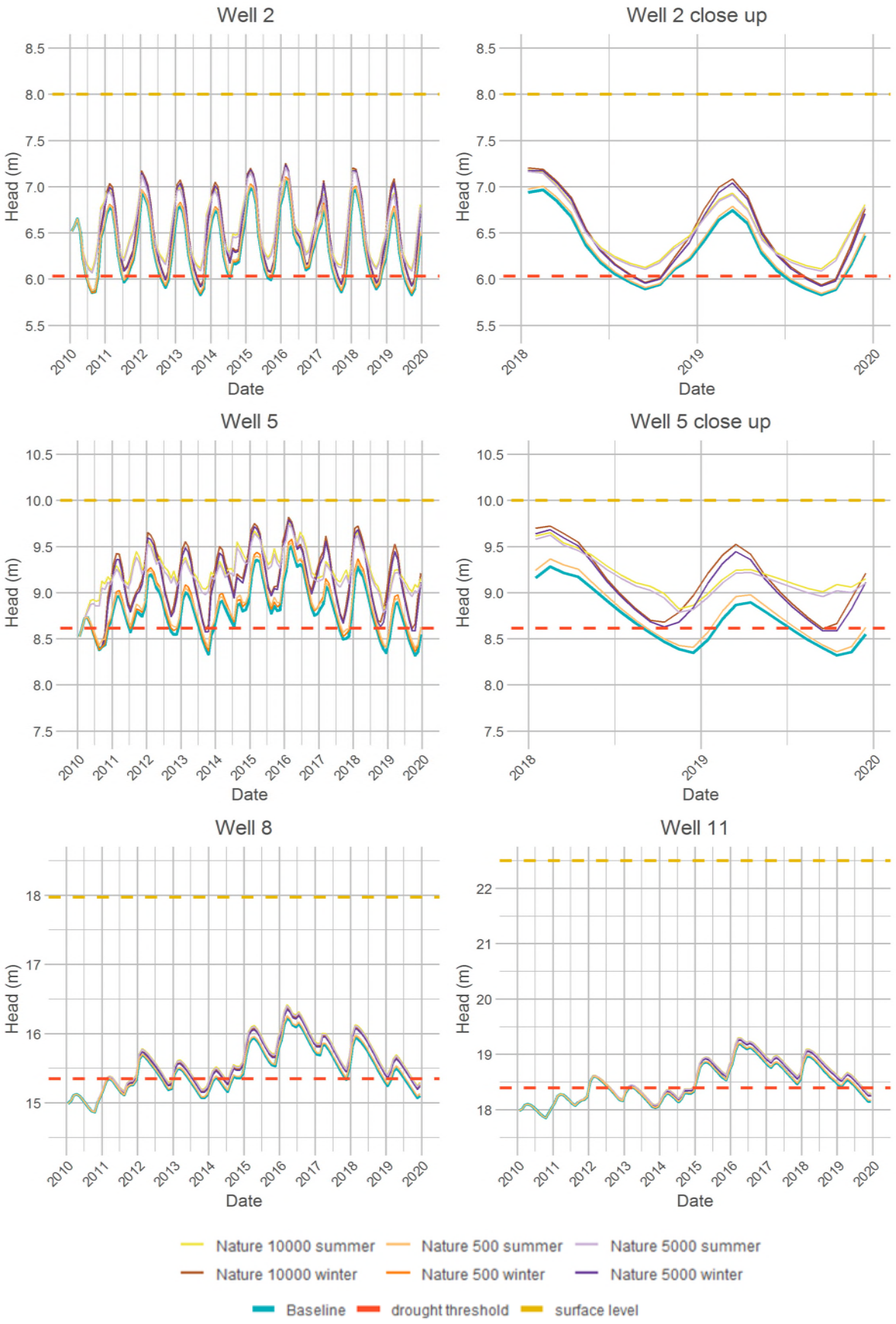

Figure 12. Comparison of the groundwater heads calculated from the baseline, MAR applied in the summer and winter in the nature area for 4 observation wells. Heads are shown in relationship to the surface level at the well location and the drought threshold level.

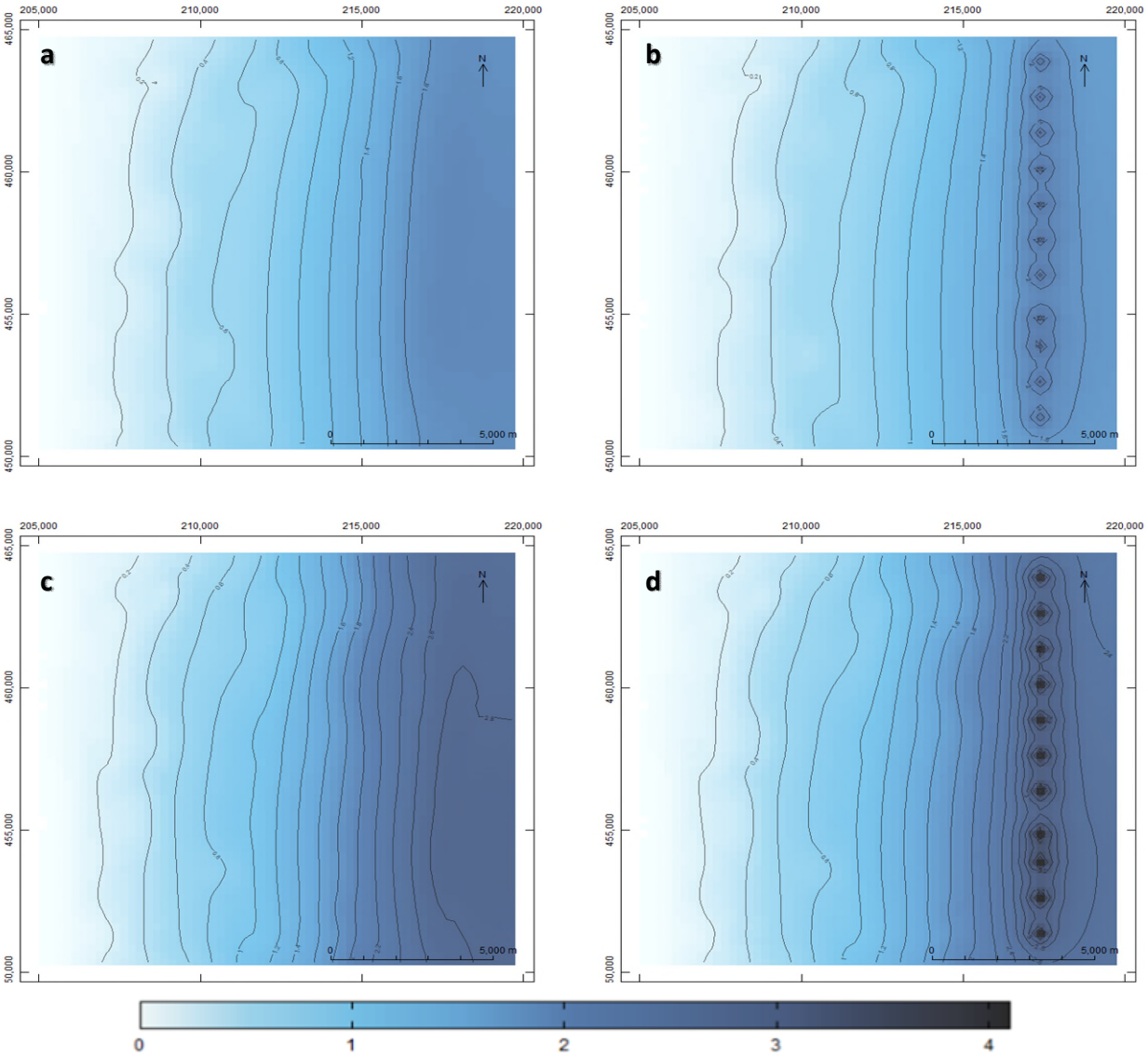

Figure 13. Change maps showing the difference in groundwater levels between AG MAR 5000s (a), AG MAR 5000w (b), AG MAR 10000s (c), AG MAR 10000w (d) and the baseline on 14-12-2018.

At well 2 only the 5000 and 10000 summer scenarios are able to prevent the droughts of 2018 and 2019, while the winter scenarios are able to alleviate them and cause a more speedy recovery. These summer scenarios are the only two able to prevent hydrological droughts because of the large recharge quantity injected at the proximity of the river. It seems that by providing so much water to the river there is a large enough buffer accumulated so that its draining capacity is saturated. This phenomenon is what explains the effectiveness of the N MAR 5000 and 10000, irrespective of summer or winter application, in preventing hydrological drought in 2018 and relieving it in 2019 at wells 8 and 11. Interestingly, the AG MAR scenarios provide a larger buffer and higher groundwater levels than N MAR scenarios, but the N MAR scenarios provide more widespread effects, reaching the entire model domain. This can also be seen by comparing Figure 13 and Figure 14: AG MAR change maps provide a greater color gradient and turns into almost white near the river, but N MAR has a constant shade of light blue that reaches over the entire model domain. A visual schematization and summary of the comparison between the effects of different MAR scenarios can be seen in Figure 15.

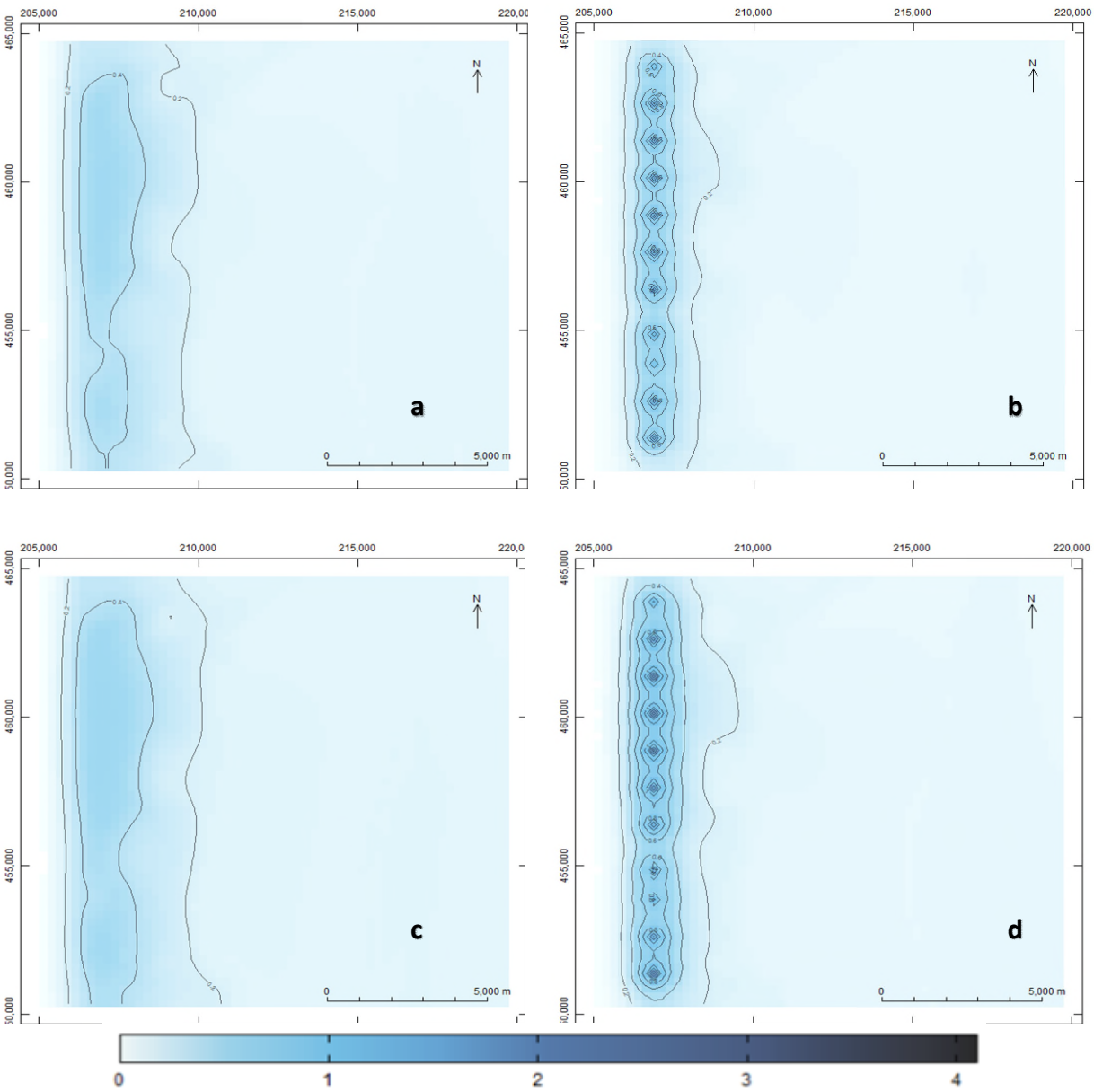

Figure 14. Change maps showing the difference in groundwater levels between N MAR 5000s (a), N MAR 5000w (b), N MAR 10000s (c), N MAR 10000w (d) and the baseline on 14-12-2018.

Table 3. Relative effect of the of each MAR scenario on preventing groundwater drought from 2015 up to and including 2019 at four observation wells. Green means that all drought episodes are avoided , yellow means may have been reached at least once but drought is less intense and the recovery is faster, and orange means that effects were too small to be significant, although they were present. The letters "s" and "w" stand for summer and winter, respectively.

Scenario	Well 2	Well 5	Well 8	Well 11
N MAR 10000 s				
N MAR 10000 w				
N MAR 5000 s				
N MAR 5000 w				
N MAR 500 s				
N MAR 500 w				
AG MAR 10000 s				
AG MAR 10000 w				
AG MAR 5000 s				
AG MAR 5000 w				
AG MAR 500 s				
AG MAR 500 w				

The effects of MAR on groundwater contribution to the river (Table 4) are consistent to what is observed at well 2. The N MAR scenarios show greater contribution in comparison to that of their corresponding AG MAR scenarios. This is consistent with the idea of the saturation of the drainage capacity of the river. In addition, contributions are greater in the summer application of each MAR scenario in comparison its corresponding winter application. This is to be expected as the river stages are lower in the summer, which increased the hydraulic gradient and, with it, groundwater flow.

Table 4. Differences between each MAR scenario and the Baseline of the mean groundwater contribution to the river during the decade of 2010 – 2019 and for only the year of 2018.

Scenario	Mean contribution 2018 (mm/d)	Mean contribution 2019 (mm/d)	Difference 2018 (mm/d)	Difference 2019 (mm/d)	% increase 2018	% increase 2019
Baseline	4.71	4.25	-	-	-	-
N MAR 10000 s	6.47	6.44	1.76	2.19	37.4	51.5
N MAR 10000 w	6.09	6.23	1.38	1.98	29.3	46.6
N MAR 5000 s	6.30	6.24	1.59	1.99	33.8	46.8
N MAR 5000 w	5.90	5.93	1.19	1.68	25.3	39.5
N MAR 500 s	4.95	4.52	0.24	0.27	5.1	6.35
N MAR 500 w	4.95	4.51	0.24	0.26	5.1	6.12
AG MAR 10000 s	5.42	5.03	0.71	0.78	15.1	18.4
AG MAR 10000 w	5.40	5.02	0.69	0.77	14.6	18.1
AG MAR 5000 s	5.22	4.84	0.51	0.59	10.8	13.9
AG MAR 5000 w	5.20	4.82	0.49	0.57	10.4	13.4
AG MAR 500 s	4.77	4.33	0.06	0.08	1.3	1.88
AG MAR 500 w	4.77	4.32	0.06	0.07	1.3	1.65

4.3.2 Effects of MAR on the vegetation

The application of MAR had less regional effect on increasing transpiration and relieving drought stress of the vegetation than in preventing hydrological drought. This was to be expected, since MAR was

applied directly to the groundwater system instead of at the soil. As with the groundwater levels, greater relative effects are to be seen at the locations nearest the injection wells (Figure 15, Figure 16, Figure 17, and Figure 18), meaning that AG MAR scenarios show more increase in both transpiration and pressure heads compared to the N MAR scenarios at locations 8 and 11 (agricultural grassland). The opposite is true for locations 2 (wetland) and 5 (natural grassland). However, unlike with groundwater levels where N MAR scenarios 5000 and 10000 had significant effects in preventing or relieving drought, their effects on the vegetation is quite low at location 2. In addition, the 500 scenarios of both N MAR and, especially, AG MAR have results to insignificant to be seen in the time series figures. Appendix I shows the remaining time series for all locations.

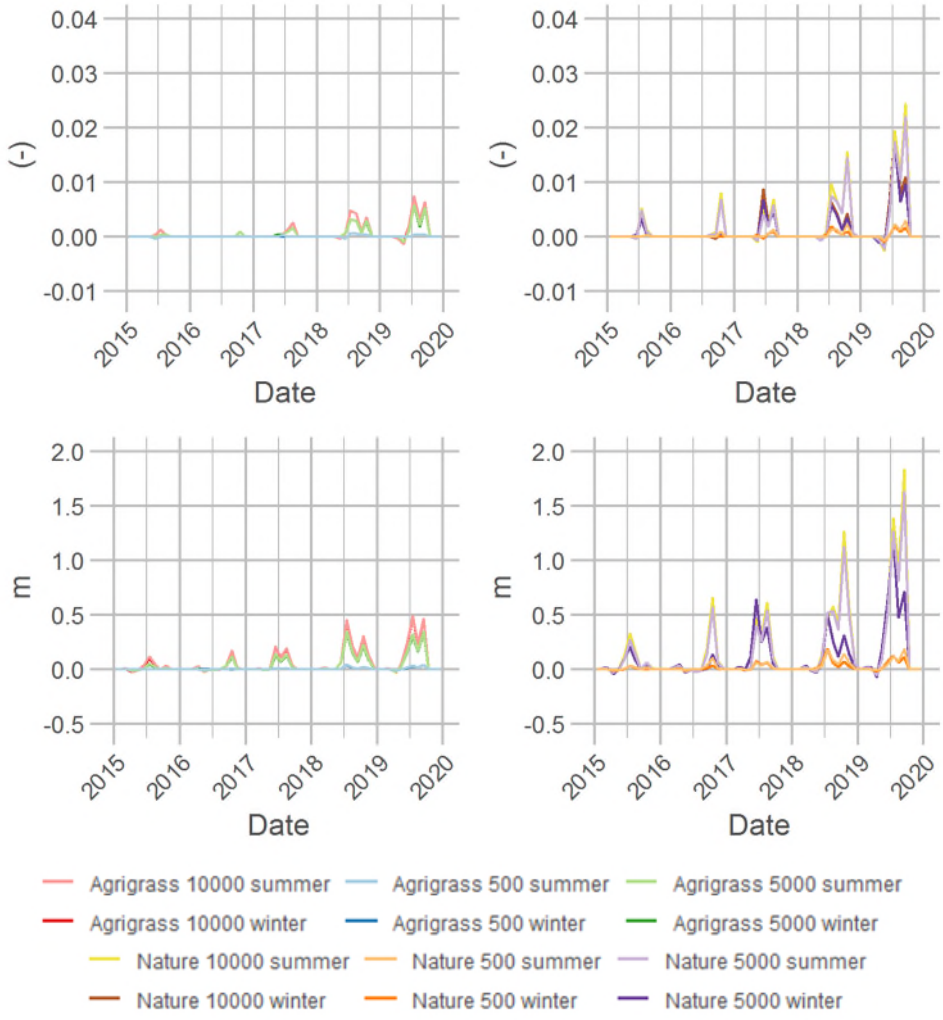

Figure 15. Difference between the MAR scenarios and the baseline regarding the relative transpiration (top row) and pressure heads (bottom row) in the root zone at location 2 (wetland) from 2015 to 2020. AG MAR and N MAR scenarios are placed in separate graphs to facilitate viewing of each time series.

At location 5, N MAR 5000 and 10000 results show a transpiration increase of about 5 and 15% in the winter and summer applications, respectively in 2018, and a 10 and 15% increase in 2019. AG MAR scenarios show an increase of about 5% in both winter and summer applications in 2018 and 2019. Pressure head increase display the same proportions: summer N MAR 5000 and 10000 cause an increase of 10 and 12 m, respectively in 2018, and 8 and 10 m in 2019. The winter application result in an increase of 5 m for both 5000 and 10000 in 2018, and between 5 and 7 m, respectively in 2019. AG MAR 5000 and 1000 both increase pressure heads by 5 m in 2018 and about 3 to 4 m in 2019.

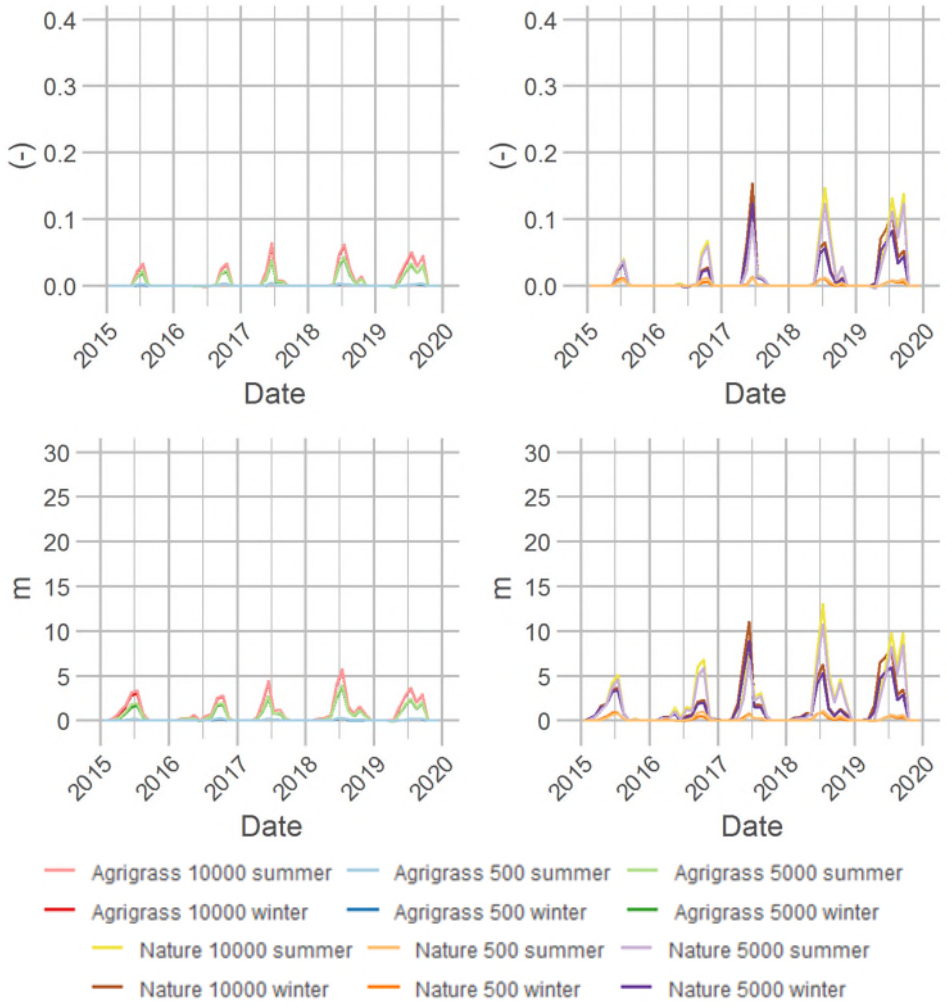

Figure 16. Difference between the MAR scenarios and the baseline regarding the relative transpiration (top row) and pressure heads (bottom row) in the root zone at location 5 (natural grassland) from 2015 to 2020. AG MAR and N MAR scenarios are placed in separate graphs to facilitate viewing of each time series.

At locations 8 and 11, the influence of N MAR scenarios is not visible anymore. Like at the previous locations, the summer and winter applications of AG MAR 5000 and 10000 have similar results to each other at location 8. Transpiration increases in 2018 around 6 and 15% in the 5000 and 10000 scenario, respectively, and about 5 and 10% in 2019. Pressure heads show an increase of 5 m in both 2018 and 2019 in the 5000 scenarios, and an increase of 10 m in 2018 and 7 m in 2019 in the 10000 scenarios.

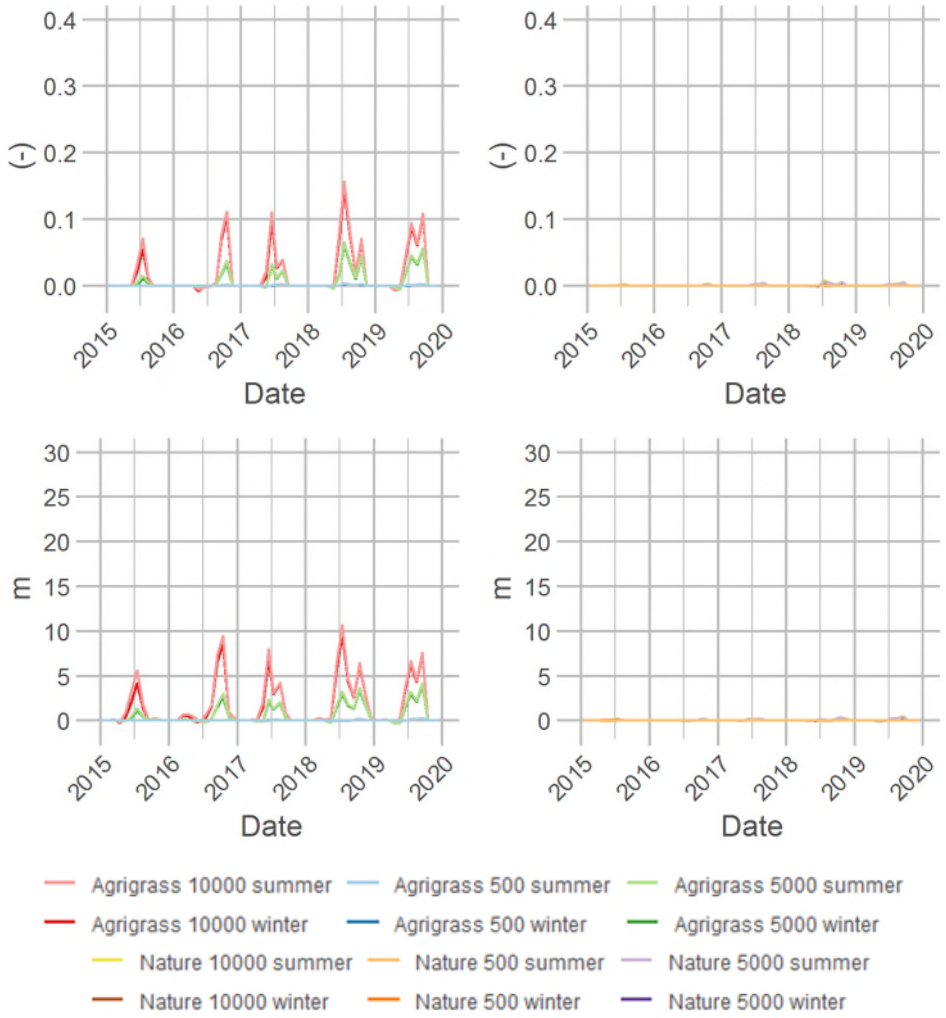

Figure 17. Difference between the MAR scenarios and the baseline regarding the relative transpiration (top row) and pressure heads (bottom row) in the root zone at location 8 (agricultural grass) from 2015 to 2020. AG MAR and N MAR scenarios are placed in separate graphs to facilitate viewing of each time series.

At location 11 a difference can be seen between the winter and summer applications of both 5000 and 10000. This is consistent with what occurs with groundwater levels at well 11, given the proximity of the injection wells. Here transpiration increases by 5 and 10% for the winter and summer 5000 scenarios, respectively, and between 20 and 75% for the 10000 scenarios in 2018. Indeed, pressure heads increase by about 4 and 5 m in the 5000 winter and summer scenarios, respectfully, while increasing by 10 and 60 m in the 10000 winter and summer scenarios. In 2019 transpiration increase is maintained for the 5000 scenarios, as are the pressure heads. The 10000 scenarios winter and summer scenarios show a 20 and 40% increase, respectively, while pressure heads increase by about 10 and 30 m.

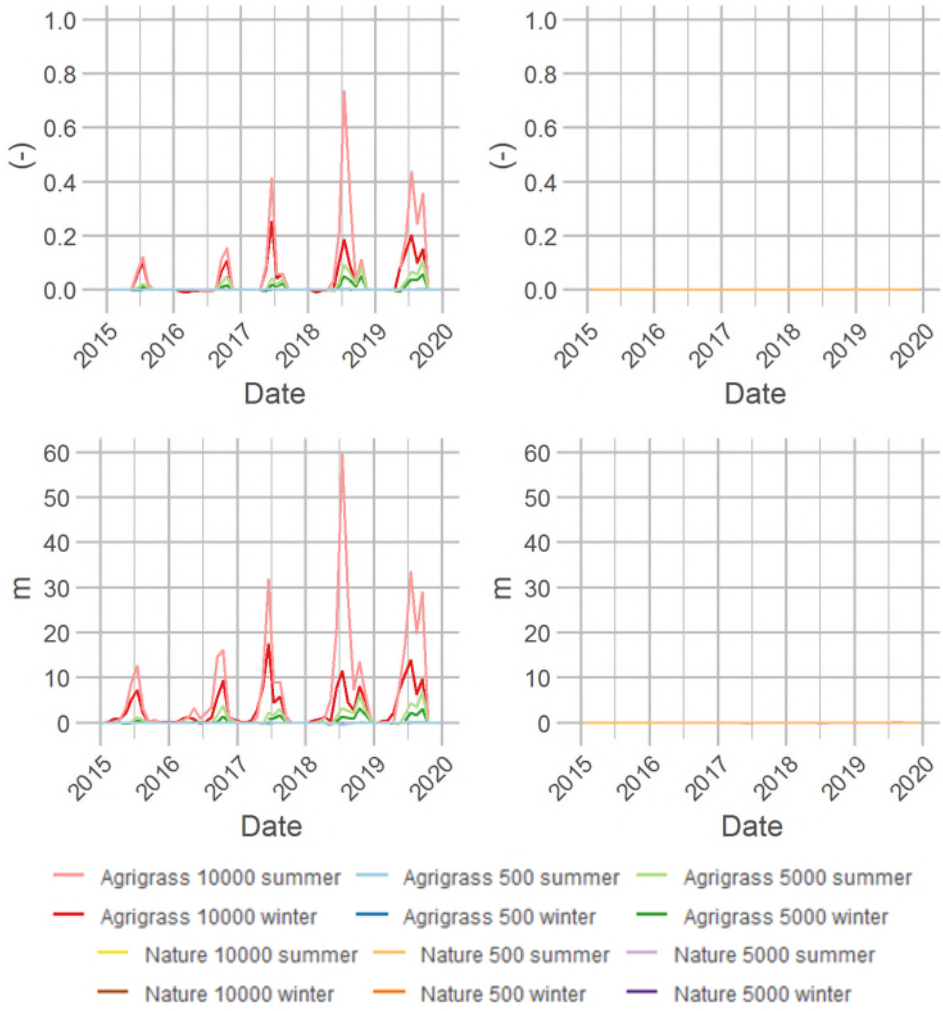

Figure 18. Difference between the MAR scenarios and the baseline regarding the relative transpiration (top row) and pressure heads (bottom row) in the root zone at location 11 (agricultural grass) from 2015 to 2020. AG MAR and N MAR scenarios are placed in separate graphs to facilitate viewing of each time series.

The spatial patterns of transpiration increase compared to the baseline during the AG MAR and N MAR scenarios can be seen in Figure 19 and Figure 20, respectively. The 500 scenarios have not been included given the small changes they produced. These figures clearly show how the AG MAR scenarios had a greater regional influence than the N MAR scenarios. In addition, it can be seen that the area where transpiration is increased the most corresponds to the seepage zone (Figure 7). Because the groundwater level is in closer to the surface in this area it is more sensitive to transpiration increase as a result of a small ground level increase.

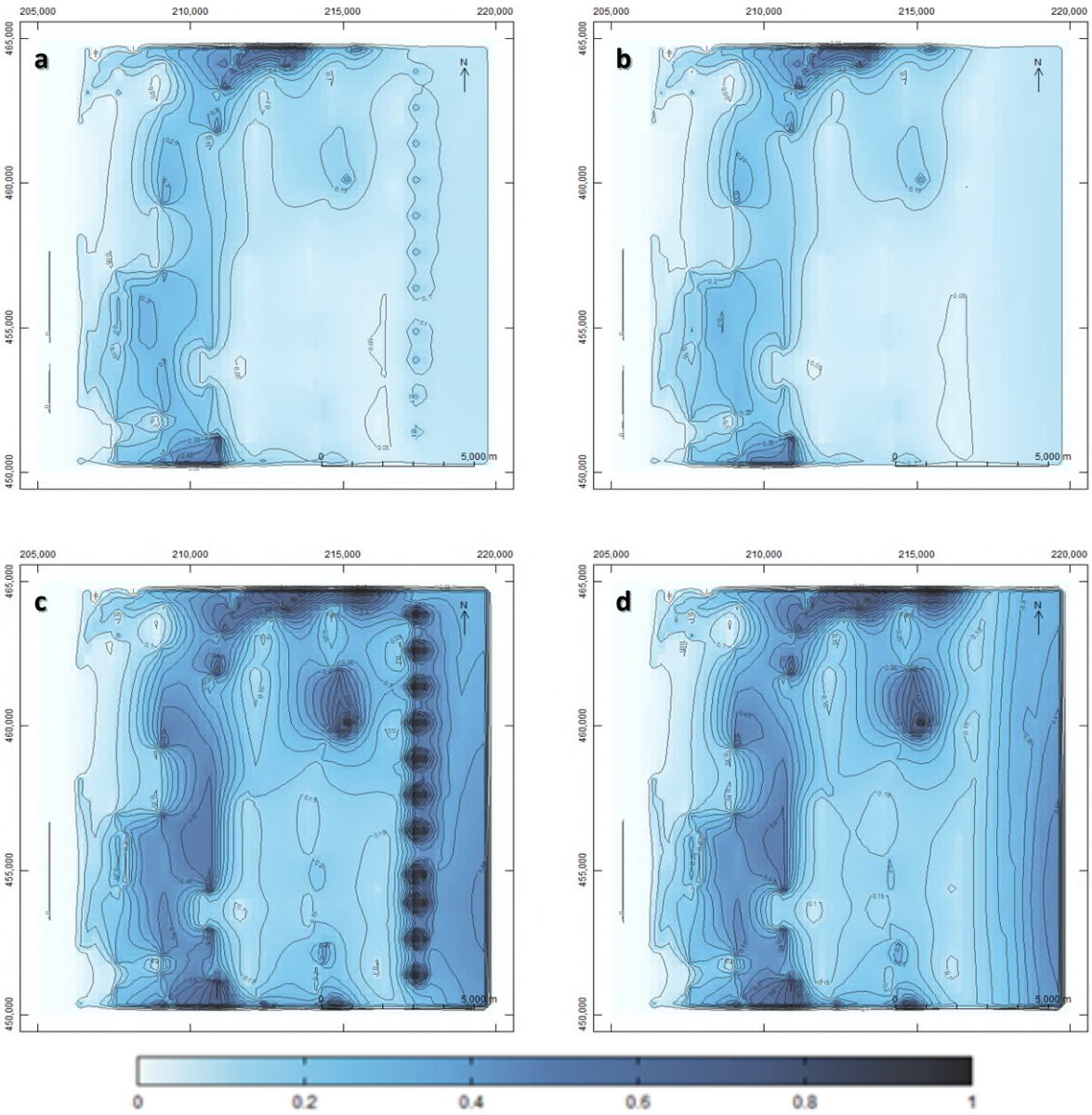

Figure 19. Change maps showing the difference in relative transpiration between AG MAR 5000s (a), AG MAR 5000w (b), AG MAR 10000s (c), AG MAR 10000w (d) and the baseline on 14-07-2018.

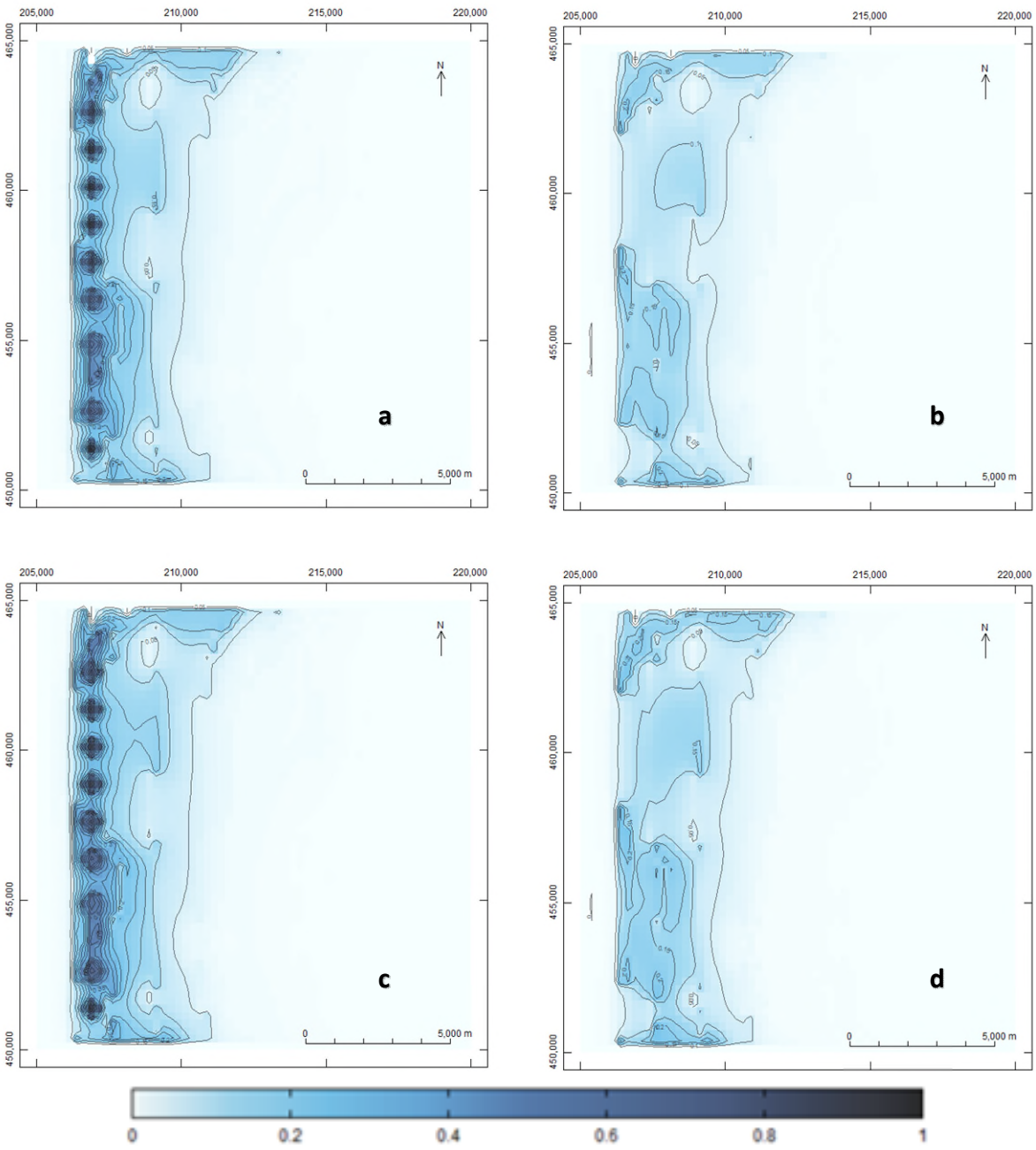

Figure 20. Change maps showing the difference in relative transpiration between N MAR 5000s (a), N MAR 5000w (b), N MAR 10000s (c), N MAR 10000w (d) and the baseline on 14-07-2018.

Table 5 shows a visual summary of the regional effects of each MAR scenario on transpiration. Effects are categorized based on the ranges of increase found in the results and the categories are not in themselves a measure of MAR effectiveness at each location. Further investigation would have to be made in order to determine what these increases mean in terms of crop yield or vegetation productivity.

Table 5. Relative effect of the of each MAR scenario on increasing relative transpiration in the summer of 2018 at four observation well locations. Dark blue means an increase in more than 15%, light blue means an increase between 5 and 15%, and pale blue means an increase in less than 5%. The letters "s" and "w" stand for summer and winter, respectively.

Scenario	Location 2	Location 5	Location 8	Location 11
Nat. 10000 s				
Nat. 10000 w				
Nat. 5000 s				
Nat. 5000 w				
Nat. 500 s				
Nat. 500 w				
Agri. grass 10000 s				
Agri. grass 10000 w				
Agri. grass 5000 s				
Agri. grass 5000 w				
Agri. grass 500 s				
Agri. grass 500 w				

5. Discussion and recommendations

In this section the assumptions regarding boundary conditions and model set up are discussed and their effects on the results are analyzed. The thesis findings are then compared to other studies on MAR and drought to contextualize them in the light of literature and current knowledge. From these considerations recommendations are made for future research and drought prevention policies are discussed.

Assumptions and model simplifications

Drought characterization

A methodological assumption made was in the characterization of droughts. Since the fixed threshold method was chosen instead of the varying threshold method, only extreme droughts were captured in this thesis. This was appropriate for the scope of the research, but choosing the former instead of the latter method can exclude the less acute drought events that occur in the winter (Sarailidis et al., 2019). Identifying droughts in the wetter months is important because it can allow for the timely prevention of these and the subsequent more severe summer droughts.

The use of threshold methods in studying hydrological drought is common practice (Eertwegh et al., 2019; Hasan et al., 2019; Sarailidis et al., 2019; Vasiliades et al., 2017), however, consideration must be given to the type of data available when establishing the thresholds. If the aim is to study drought

preventive measures in natural ecosystems as a way to recover their natural conditions, it is evident that data will give an indication of a drought threshold in an already heavily modified environment (Hendriks et al., 2014; Vissers & van der Perk, 2008). In the thesis the drought threshold was calculated based on groundwater level frequency curves, meaning that MAR effectiveness was measured against relative drought instead of an established minimum. The application of MAR might be judged less effective if a targeted minimum groundwater level for ecological purposes is above the 80% exceedance probability. Nevertheless, the use of the threshold method was appropriate for this thesis since it was a preliminary analysis on the effects of MAR through injections wells for natural (and agricultural) ecosystems in an already modified environment.

River boundary conditions

Constant seasonal river stages for the summer and winter were adopted in the model. Because these boundary conditions were assumed to be unchanging, it was possible to conduct a modeling experiment to directly test the sensitivity of groundwater levels, soil moisture pressure heads and transpiration without the intervention of other processes occurring in the system. However, such constant values in river stages are seldom the reality. Precipitation determines river flows and levels much more immediately than groundwater, thus in a dry year river stages should be lower than in wetter years. This thesis model's river is based on the IJssel the which stages reached 5.35 m above NAP during the beginning of 2018 and values as low as 0.93 m at the end of August 2018 at Deventer (Rijkswaterstaat, 2020). The difference of more than 4 meters between these values is more than double the difference between the winter and summer model river stages. By not considering more extreme values in river stages and all variability between them in the research means that the effects of MAR application in wetter winters could have been enhanced by higher river stages and possibly flooding of the wetland area. Conversely MAR application in particularly dry summers could be more limited by lower river stages.

Nevertheless, model results give an indication of the relative regional effects of the different MAR scenarios in the model, and hence are valid for the scope of this research. Future studies focusing on the actual effectiveness of MAR in situations of varying drought strength would need to apply more complex models with transient river conditions.

Drainage conditions

Another assumption made was that the model, without the presence of other rivers or drainages systems, is representative of areas with a higher drainage density. The model bears the characteristics of the cover sand landscape of the Pleistocene uplands in terms of geology, but it resembles the moraines landscape in terms of drainage density (Jalink & van Doorn, 2017). In the model the boundary conditions and the lack of drainage create a situation where groundwater level isoclines are fairly parallel to each other, and therefore also the flow paths. This condition probably maximizes the extent of the MAR effects in the model domain, as it is one large groundwater system (Vissers & van der Perk, 2008). However, in reality drainage density in most of the Pleistocene uplands is much higher, which changes the flow patterns and travel distances of groundwater (Vissers & van der Perk, 2008).

Soil representation

The model domain was much simplified by the use of a uniform soil cover, which is far from the reality seen in the Achterhoek. A heterogeneous soil cover would have affected the spatial pattern of MAR effect on relative transpiration and soil moisture pressure head. Heterogeneities in soil cause differences in relationships between pressure heads and soil moisture, and thus in soil water retention (Brooks & Corey, 1966). Therefore, the thesis results have to be taken as indicative of the magnitude of the regional effects.

Comparison to existing MAR studies – Impact on groundwater levels

Even with the presence of assumptions and great simplifications, the model results are in line with literature on the use of MAR injection wells for increasing groundwater levels. Holländer et al. (2009), modeled the use of ASR-wells for sustainable groundwater management considering a series of confined coastal aquifers in Eastern India. They found that in an area of 15 ha, an area 1400 times smaller than the one modeled in this thesis, one ASR-well infiltrating 218 mm/year was enough to allow for sustainable groundwater withdrawal. The amount infiltrated by the one well is more than twice the amount infiltrated for the entire well field in this model. However, the scopes for applying MAR in their study (allow for sustainable groundwater withdrawal) is different from the scope of this thesis, explaining the differences in amount of water infiltrated.

Valley et al. (2006) performed a modeling experiment to explore the effects of MAR in the sandy and unconfined Prato aquifer, Italy, as measures to replenish its overexploited groundwater. In two of the simulations, wells injected a total of 400 l/s (approximately 34,560 m^3/d) during 8 months of the year, totaling 12.6 million m^3. This volume is the same order of magnitude as the MAR 10000 scenarios (19.8 million m^3 in a year). In the simulation by these authors, water was taken from the Bisenzio river and was less than 10% of its average flow of 5.1 m^3/s. In the MAR 10000 scenarios the infiltration of 1.27 m^3/s was only 0.3% of the river IJssel's average discharge of 419 m^3/s for 2018 (Rijkswaterstaat, 2020). Simulations by Valley et al. (2006) with injection wells in different locations resulted in a groundwater level increase of 8 meters from their baseline scenario close to the injection wells and 2 meters about 5 km from them. The MAR 10000 scenarios in the agricultural grass area resulted in approximately 3 meters increase from the baseline close to the injection wells and 1.25 m about 5 km away from them. Comparing the regional effects of both MAR applications, both have similar results, given the different groundwater systems.

Comparison to existing MAR studies – Impact on vegetation

The effects of the results of the MAR scenarios on the vegetation are comparable to other studies. Niswonger et al. (2017) found that applying off-season irrigation in a hypothetical river basin model representative of the semiarid western United States produced an increase in water consumption of 7 to 13% for crops and 20 to 30% for natural vegetation. Eertwegh et al. (2019), using the LHM version 3.4 which also contain iMOD and MetaSWAP (Bos-Burgering et al., 2018), found that the increase of all drainage ditches and channels in specific areas of the Pleistocene uplands produced an increase in transpiration between 10 and 15% between July 21 and August 10, 2018. The N MAR 5000 and 10000 results show similar values in July 2018, obtaining between 5 and 15% transpiration increase in most of the region, especially for the injection wells located in the agricultural grassland area.

Potential for future MAR applications

In all, the results of this thesis are conclusive enough to support the claim that MAR does seem to have a regional effect in preventing hydrological drought, and the potential for increasing transpiration in natural and agricultural vegetation in the Pleistocene uplands. A potential is seen for increasing transpiration because the effects of MAR for this aim were not as widespread as for the aim of preventing hydrological drought. In order to increase it, further modeling experimental research could be done with greater well discharges in the agricultural area, or by combining the application of other MAR techniques with the injection wells.

Combinations would probably be more effective by tailoring them to the location. For the specific case of this thesis' model domain, increasing river stages and applying water spreading methods such as infiltration basins in the wetland area could reduce the impact of river drainage on the groundwater levels, indirectly increasing transpiration in the agricultural grassland, and directly increase transpiration of the natural vegetation. Specific locations in the Pleistocene uplands would need to be treated differently due to inherent heterogeneities, but perhaps the most important technique to be combined

with injections wells remains increasing water levels of drainage systems at the same time of decreasing their discharge (Eertwegh et al., 2019). The N MAR 5000 and 10000 results support this idea since groundwater levels were raised close to the river, allowing for more widespread effects in the model domain.

Impact on land use

Connected to this idea is the value of the role of natural ecosystems in MAR application. Allowing space for natural vegetation in areas where groundwater levels are naturally high ensure the stability of the groundwater system (Jalink & van Doorn, 2017). Instead, by allocating other human uses that need a controlled minimum groundwater depth, such as agriculture, these areas may become excessively drained (Jalink & van Doorn, 2017). Given the geohydrological characteristics of the Pleistocene Uplands this leads to rapid dewatering of aquifers, explaining the rapid onset of the hydrological drought of 2018 after a very wet autumn and winter.

From the model results, it can be inferred that natural vegetation has a role in the effectiveness of MAR application. Ecological dynamics ensure that natural ecosystems become adapted to the environment they are in, meaning that preventing oxygen stress for natural vegetation in areas of high groundwater level is not an issue. However, ensuring enough oxygen in the root zone is important for most agricultural crops, making them not adapted to these locations. The model built shows how the effects of MAR are negligible close to the river because of its low stages compared to the surface level. By keeping stages seasonably fixed, the river functions more like drainage does in reality. If the stages were to be increased to near the root zone, this would not be a problem for natural ecosystems, but would be a problem for agriculture.

On the other hand, if crops were placed at the seepage zone of the model and drainage was applied in this area to make this possible, the effectiveness of MAR would have been decreased. Thus, in order to maximize the regional effects of MAR, it is important to allow the spatial distribution of groundwater levels to follow their natural course, instead of applying drainage where its effects can still be noticed. Consequences of combining different MAR systems and combining MAR measures with natural vegetation for policy making include the need to closely consider these in the land use planning process. With different areas allocated to recharge, the necessity of multiple MAR techniques substantiate the relevance of including spatial planning when designing measures for preventing drought.

Human influence drainage

Another finding which supports the perception that excessive drainage in the Pleistocene uplands is linked to the fast development of hydrological drought was found during the model calibration. The fact that the hydraulic conductivity of the third layer had to be increased compared to original estimates to provide enough drainage in the model and keep groundwater levels under the surface level is an indication of the impact that drainage systems have on overall water availability in the Achterhoek region and the Pleistocene uplands in general (Hendriks et al., 2014; Kloosterman et al., 1995; Plag, 2020; A. van Loon et al., 2014; Vissers & van der Perk, 2008). This adds to the discussion on the need to reduce groundwater drainage in order to increase local groundwater availability (Eertwegh et al., 2019; Plag, 2020; Ritzema & Stuyt, 2015; A. van Loon et al., 2014) and raise questions of whether hydrological drought would have developed in the first place if less drainage practices had been adopted. Future modeling research with the model in this thesis could include a sensitivity analysis of added drainage systems to determine how intensely the hydrological drought of 2018 and 2019 would have developed.

Considering the reflections above, further implications for future research, water management and land use policy in the Pleistocene uplands are linked to the principle of 'drought determines functions' (STOWA, 2013; Verdonschot, 2010). This principle recognizes the need for land use planning that contributes to groundwater retention, and MAR-nature systems could be developed in this line of

thinking. Since there are still knowledge gaps present regarding the effectiveness of applying this principle to land use management (STOWA, 2013), further research could combine the application of MAR systems and targeted land use conversion to nature.

6. Conclusion

The purpose of this thesis was to identify the regional effects of locally applied managed aquifer recharge, as a drought preventive measure, on natural and agricultural ecosystems in the Pleistocene uplands of the Netherlands. The hypothetical model results suggest that injection wells, the chosen MAR technique, does have regional effects when preventing hydrological drought. The 12 MAR scenarios had varying success in increasing groundwater levels in periods where the baseline scenario suffered hydrological drought: N MAR 5000 and 10000 had effects in the entire model domain, preventing hydrological drought in half of its extension for the summer application. Both winter and summer applications of AG MAR 5000 and 10000 had effects in almost the entire domain except for near the river, preventing hydrological drought in half of the domain. The MAR 500 scenarios had less effects. They reached half of the model domain when applied in the agricultural area, preventing hydrological drought at the injection well location (both winter and summer), and had insignificant effects when applied at the nature area due to proximity of the river.

The effects on increasing transpiration during drought stress episodes was less in extent. The scenarios where injection wells applied 500m^3/d recharge showed less than 5% increase in the entire domain. In the N MAR 5000 and 10000 scenarios, 5% increase was seen in almost the entire model domain, while at the location of the injection wells transpiration increased between 5 and 10%. In the AG MAR 5000 and 10000 scenarios, effects were more significant: with 10000 m^3/d, transpiration increased more than 15% in the vicinity of the injection wells with increases between 5 and 10% for the rest of the model domain except for near the river. When 5000 m^3/d was applied, the half of the domain closest to the injection wells showed transpiration increase between 5 and 10%.

The findings of this thesis underline that combining injection wells with other MAR techniques, especially drainage level increase in order to decrease groundwater discharge, can improve the effectiveness of MAR in preventing drought. This implies the need for implementing drought preventive measures that not only consider technical solutions but land use planning as well.

References

Alvarez, J., & Estrela, T. (2000). Socio-economic drought. In H. Hisdal & L. M. Tallaksen (Eds.), *Drought event definition: ARIDE technical report no. 6* (pp. 16–17). University of Oslo. https://www.droughtmanagement.info/literature/UNIVERSITYofOSLO_Drought_Event_Definition_2000.pdf

Aqueduct Water Risk Atlas. (2019). https://www.wri.org/applications/aqueduct/water-risk-atlas/#/?advanced=false&basemap=hydro&indicator=drr_cat&lat=48.74170087976542&lng=-4.658203125000001&mapMode=view&month=1&opacity=0.5&ponderation=DEF&predefined=false&projection=absolute&scenario=optimi

Bos-Burgering, L., Hunink, J., Veldhuizen, A., Walsum, P. van, Prinsen, G., Pouwels, J., & Kroon, T. (2018). *Veranderingsrapportage LHM 3.4.0; ontwikkelingen ten behoeve van landelijke analyse van de zoetwatervoorziening 2018*. http://www.nhi.nu/nl/files/7915/4152/2765/11202224-003-BGS-0001-v5-r-Veranderingsrapportage_LHM_3.4.0-def_-_aanpassing_nov_2018_-_DEF.pdf

Brooks, R. H., & Corey, A. T. (1966). Properties of porous media affecting fluid flow. *Journal of the Irrigation and Drainage Division*, *9*(2), 61–90. https://www.wipp.energy.gov/information_repository/cra/CRA-2014/References/Others/Brooks_Corey_1964_Hydraulic_Properties_ERMS241117.pdf

Dashora, Y., Dillon, P., Maheshwari, B., Soni, P., Dashora, R., Davande, S., Purohit, R. C., & Mittal, H. K. (2018). A simple method using farmers' measurements applied to estimate check dam recharge in Rajasthan, India. *Sustainable Water Resources Management*, *4*(2), 301–316. https://doi.org/10.1007/s40899-017-0185-5

De Mulder, E. F. J. (2019). Landscapes. In *The Netherlands and the Dutch* (World Regi, pp. 35–58). Springer, Cham. https://doi.org/10.1007/978-3-319-75073-6_3

de Vries, J. J. de, & van Rees Veilinga, E. (1972). Buried channel aquifers and present open drainage system of East Gelderland, the Netherlands. *Geologie En Mijnbouw*, *51*(1), 45–52. https://library.wur.nl/WebQuery/wurpubs/fulltext/320475

Deltares. (2019). *iMOD 5.0* (5.0). Deltares. https://oss.deltares.nl/web/imod/home

Dillon, P., Pavelic, P., Palma Nava, A., & Weiping, W. (2018). Advances in multi-stage planning and implementing managed aquifer recharge for integrated water management. *Sustainable Water Resources Management*, *4*(2), 145–151. https://doi.org/10.1007/s40899-018-0242-8

Dillon, P., Stuyfzand, P., Grischek, T., Lluria, M., Pyne, R. D. G., Jain, R. C., Bear, J., Schwarz, J., Wang, W., Fernandez, E., Stefan, C., Pettenati, M., van der Gun, J., Sprenger, C., Massmann, G., Scanlon, B. R., Xanke, J., Jokela, P., Zheng, Y., … Sapiano, M. (2019). Sixty years of global progress in managed aquifer recharge. *Hydrogeology Journal*, *27*(1), 1–30. https://doi.org/10.1007/s10040-018-1841-z

Eertwegh, G. A. P. H. van den, Bartholomeus, R. P., Louw, P. de, Witte, J. P. M., Dam, J. van, Deijl, D. van, Hoefsloot, P., Clevers, S. H. P., Hendriks, D., & al., et. (2019). *Droogte in zandgebieden van Zuid-, Midden- en Oost-Nederland. Rapportage Fase 1: ontwikkeling van uniforme werkwijze voor analyse van droogte en tussentijdse bevindingen*. https://library.kwrwater.nl/publication/60038685/

Fleuchaus, P., Godschalk, B., Stober, I., & Blum, P. (2018). Worldwide application of aquifer thermal energy storage – A review. *Renewable and Sustainable Energy Reviews*, *94*, 861–876. https://doi.org/10.1016/j.rser.2018.06.057

Göbel, P., Stubbe, H., Weinert, M., Zimmermann, J., Fach, S., Dierkes, C., Kories, H., Messer, J., Mertsch, V., Geiger, W. F., & Coldewey, W. G. (2004). Near-natural stormwater management and its effects on the water budget and groundwater surface in urban areas taking account of the hydrogeological conditions. *Journal of Hydrology*, *299*(3–4), 267–283. https://doi.org/10.1016/j.jhydrol.2004.08.013

Guo, Z., Xiao, X., & Li, D. (2000). An assessment of ecosystem services: water flow regulation and hydroelectric power production. *Ecological Applications*, *10*(3), 925–936. https://doi.org/10.1890/1051-0761(2000)010[0925:AAOESW]2.0.CO;2

H2O. (2018). *Langdurige natte periode legt problemen met grondwater bloot*. https://www.h2owaternetwerk.nl/h2o-actueel/langdurige-natte-periode-legt-problemen-met-grondwater-bloot

Haddeland, I., Clark, D. B., Franssen, W., Ludwig, F., Voß, F., Arnell, N. W., Bertrand, N., Best, M., Folwell, S., Gerten, D., Gomes, S., Gosling, S. N., Hagemann, S., Hanasaki, N., Harding, R., Heinke, J., Kabat, P., Koirala, S., Oki, T., … Yeh, P. (2011). Multimodel estimate of the global terrestrial water balance: Setup and first results. *Journal of Hydrometeorology*, *12*(5), 869–884. https://doi.org/10.1175/2011JHM1324.1

Harbaugh, A. W. (2005). *MODFLOW-2005, The U.S. Geological Survey Modular Ground-Water Model—the Ground-Water Flow Process*. https://pubs.usgs.gov/tm/2005/tm6A16/PDF.htm

Hasan, H. H., Mohd Razali, S. F., Muhammad, N. S., & Ahmad, A. (2019). Research Trends of Hydrological Drought: A Systematic Review. *Water*, *11*(11), 2252. https://doi.org/10.3390/w11112252

He, X., Wada, Y., Wanders, N., & Sheffield, J. (2017). Intensification of hydrological drought in California by human water management. *Geophysical Research Letters*, *44*(4), 1777–1785. https://doi.org/10.1002/2016GL071665

Hendriks, D. M. D., Kuijper, M. J. M., & van Ek, R. (2014). Groundwater impact on environmental flow needs of streams in sandy catchments in the Netherlands. *Hydrological Sciences Journal*, *59*(3–4), 562–577. https://doi.org/10.1080/02626667.2014.892601

Holländer, H. M., Mull, R., & Panda, S. N. (2009). A concept for managed aquifer recharge using ASR-wells for sustainable use of groundwater resources in an alluvial coastal aquifer in Eastern India. *Physics and Chemistry of the Earth*, *34*(4–5), 270–278. https://doi.org/10.1016/j.pce.2008.05.001

IenM. (2015). *National Water Plan 2016-2021*. https://www.government.nl/documents/policy-notes/2015/12/14/national-water-plan-2016-2021

IPCC. (2014). *Climate Change 2014: Synthesis Report. Contribution of Working Groups I, II and III to the Fifth Assessment Report of the Intergovernmental Panel on Climate Change [Core Writing Team, R.K. Pachauri and L.A. Meyer (eds.)]*. https://www.ipcc.ch/site/assets/uploads/2018/02/SYR_AR5_FINAL_full.pdf

Jalink, M., & van Doorn, A. (2017). *Functiecombinatie waterwinning en natuur: verkenning in drie landschapstypen, BTO rapport 2017.022*.

James Dennedy-Frank, P., & Gorelick, S. M. (2019). *Insights from watershed simulations around the world: Watershed service-based restoration does not significantly enhance streamflow*. https://doi.org/10.1016/j.gloenvcha.2019.101938

Kasse, C. (1997). Cold-climate aeolian sand-sheet formation in North-Western Europe (c. 14-12.4 ka); a response to permafrost degradation and increased aridity. *Permafrost and Periglacial Processes*, *8*(3), 295–311. https://doi.org/10.1002/(SICI)1099-1530(199709)8:3<295::AID-PPP256>3.0.CO;2-0

Kloosterman, F. H., Stuurman, R. J., & van der Meijden, R. (1995). Groundwater flow systems analysis on a regional and nation-wide scale in the Netherlands; the use of flow systems analysis in wetland management. *Water Science and Technology*, *31*(8), 375–378. https://doi.org/10.2166/wst.1995.0333

KNMI. (2019a). *Is de droogte eindelijk voorbij?* https://www.knmi.nl/over-het-knmi/nieuws/is-de-droogte-eindelijk-voorbij

KNMI. (2019b). *Klimaatdata en advies [Precipitation and evapotranspiration data from the Deelen meteorological station]*. http://projects.knmi.nl/klimatologie/daggegevens/selectie.cgi

Kramer, N., Mens, M., Beersma, J., & Kielen, N. (2019). *Hoe extreem was de droogte van 2018?* https://www.h2owaternetwerk.nl/vakartikelen/hoe-extreem-was-de-droogte-van-2018

Margariti, J., Rangecroft, S., Parry, S., Wendt, D. E., & Van Loon, A. F. (2019). Anthropogenic activities alter drought termination. *Elem Sci Anth*, *7*(1), 27. https://doi.org/10.1525/elementa.365

Marx, A., Kumar, R., Thober, S., Rakovec, O., Wanders, N., Zink, M., Wood, E. F., Pan, M., Sheffield, J., & Samaniego, L. (2018). Climate change alters low flows in Europe under global warming of 1.5, 2, and 3 °C. *Hydrology and Earth System Sciences*, *22*(2), 1017–1032. https://doi.org/10.5194/hess-22-1017-2018

Mauck, B. A., Winter, K., & Wolski, P. (2017). *The capacity of the Cape Flats aquifer and its role in water sensitive urban design in Cape Town (Ph.D)* [University of Cape Town]. https://open.uct.ac.za/handle/11427/27293

Mishra, A. K., & Singh, V. P. (2010). A review of drought concepts. In *Journal of Hydrology* (Vol. 391, Issues 1–2, pp. 202–216). Elsevier. https://doi.org/10.1016/j.jhydrol.2010.07.012

Mooers, E. W., Jamieson, R. C., Hayward, J. L., Drage, J., & Lake, C. B. (2018). Low-Impact Development Effects on Aquifer Recharge Using Coupled Surface and Groundwater Models. *Journal of Hydrologic Engineering*, *23*(9), 04018040. https://doi.org/10.1061/(ASCE)HE.1943-5584.0001682

Niswonger, R. G., Morway, E. D., Triana, E., & Huntington, J. L. (2017). Managed aquifer recharge through off-season irrigation in agricultural regions. *Water Resources Research*, *53*(8). https://doi.org/10.1002/2017WR020458

Pauw, P. S., van Baaren, E. S., Visser, M., de Louw, P. G. B., & Oude Essink, G. H. P. (2015). Increasing a freshwater lens below a creek ridge using a controlled artificial recharge and drainage system: a case study in the Netherlands. *Hydrogeology Journal*, *23*(7), 1415–1430. https://doi.org/10.1007/s10040-015-1264-z

PDOK. (2012). *Actueel Hoogtebestand Nederland 1*. Nationaal Georegister. https://www.pdok.nl/viewer/

Peters, E. (2003). *Propagation of drought through groundwater systems Illustrated in the Pang (UK) and Upper-Guadiana (ES) catchments* [Wageningen University]. https://library.wur.nl/WebQuery/wurpubs/fulltext/121490

Peters, L., & van Lanen, H. (2000). Hydrological drought - groundwater. In H. Hisdal & L. Tallaksen (Eds.), *Drought Event Definition: ARIDE Technical Report No. 6* (pp. 16–17). University of Oslo. https://www.droughtmanagement.info/literature/UNIVERSITYofOSLO_Drought_Event_Definition_2000.pdf

Plag, G. (2020). *Interview N. Wanders en R.P. Bartholomeus over droogte probleem in Nederland (15 July)*. NPO Radio 1. https://www.nporadio1.nl/spraakmakers/onderwerpen/61806-2020-07-15-niko-wanders-en-ruud-bartholomeus-over-droogte-probleem-in-nederland

Rijkswaterstaat. (2020). *Waterinfo*. https://waterinfo.rws.nl/#!/nav/index/

Ringleb, J., Sallwey, J., & Stefan, C. (2016). Assessment of Managed Aquifer Recharge through Modeling—A Review. *Water*, *8*(12), 579. https://doi.org/10.3390/w8120579

Ritzema, H. P., & Stuyt, L. C. P. M. (2015). Land drainage strategies to cope with climate change in the Netherlands. *Acta Agriculturae Scandinavica, Section B — Soil & Plant Science*, *65*(sup1), 80–92. https://doi.org/10.1080/09064710.2014.994557

rtv Oost. (2018). *Enschede peinst er niet over om grondwater in Enschede-Noord weg te pompen*. https://www.rtvoost.nl/nieuws/284583/Enschede-peinst-er-niet-over-om-grondwater-in-Enschede-Noord-weg-te-pompen

Samaniego, L., Thober, S., Kumar, R., Wanders, N., Rakovec, O., Pan, M., Zink, M., Sheffield, J., Wood, E. F., & Marx, A. (2018). Anthropogenic warming exacerbates European soil moisture droughts. *Nature Climate Change*, *8*(5), 421–426. https://doi.org/10.1038/s41558-018-0138-5

Sarailidis, G., Vasiliades, L., & Loukas, A. (2019). Analysis of streamflow droughts using fixed and variable thresholds. *Hydrological Processes*, *33*(3). https://doi.org/10.1002/hyp.13336

Sari Kovats, R., Valentini, R., Bouwer, L. M., Georgopoulou, E., Jacob, D., Martin, E., Rounsevell, M., Soussana, J.-F., Beniston, M., Kajfez Bogataj, L., Corobov, R., Vallejo, R., Valentini, R., Bouwer, L., Georgopoulou, E., Jacob, D., Martin, E., Rounsevell, M., Soussana, J., … White, L. (2014). Europe. In *Climate Change 2014: Impacts, Adaptation, and Vulnerability* (pp. 1270, 1276, 1279). Cambridge University Press. https://www.ipcc.ch/site/assets/uploads/2018/02/WGIIAR5-Chap23_FINAL.pdf

Scanlon, B. R., Reedy, R. C., Faunt, C. C., Pool, D., & Uhlman, K. (2016). Enhancing drought resilience with conjunctive use and managed aquifer recharge in California and Arizona. *Environ. Res. Lett*, *11*(3), 49501. https://doi.org/10.1088/1748-9326/11/4/049501

Schokker, J., Weerts, H. J. T., Westerhoff, W. E., Berendsen, H. J. A., & den Otter, C. (2007). Introduction of the boxtel formation and implications for the quaternary lithostratigraphy of the Netherlands. *Geologie En Mijnbouw/Netherlands Journal of Geosciences*, *86*(3), 197–210. https://doi.org/10.1017/s0016774600077805

Schokker, Jeroen, & Koster, E. A. (2004). Sedimentology and Facies Distribution of Pleistocene Cold-climate Aeolian and Fluvial

Deposits in the Roer Valley Graben (Southeastern Netherlands). *Permafrost and Periglacial Processes*, *20*(November 2002), 1–20. https://doi.org/10.1002/ppp.477

Sprenger, C., Hartog, N., Hernández, M., Vilanova, E., Grützmacher, G., Scheibler, F., & Hannappel, S. (2017). Inventory of managed aquifer recharge sites in Europe: historical development, current situation and perspectives. *Hydrogeology Journal*, *25*(6), 1909–1922. https://doi.org/10.1007/s10040-017-1554-8

Stefan, C., & Ansems, N. (2018). Web-based global inventory of managed aquifer recharge applications. *Sustainable Water Resources Management*, *4*, 153–162. https://doi.org/10.1007/s40899-017-0212-6

Sterk, M., & Wamelink, W. (2019). Case study de droogte van 2018 op zoek naar een succesvolle systeemaanpak om te reageren op droogte. *Water Governance*, *2*, 57–60. https://library.wur.nl/WebQuery/wurpubs/fulltext/498512

STOWA. (2013). *Drought determines functions*. https://www.stowa.nl/deltafacts/zoetwatervoorziening/delta-facts-english-versions/drought-determines-functions

TNO. (2013). *Lithostratigrafische Nomenclator van de Ondiepe Ondergrond, versie 2013*. https://www.dinoloket.nl/en/nomenclator-ondiep

TNO. (2017). *Subsurface models| DINOloket*. https://www.dinoloket.nl/en/subsurface-models

TNO. (2019). *DINO/BRO Well with research data*. TNO. https://www.dinoloket.nl/en/subsurface-data

Valiya Veettil, A., & Mishra, A. k. (2020). Multiscale hydrological drought analysis: Role of climate, catchment and morphological variables and associated thresholds. *Journal of Hydrology*, *582*, 124533. https://doi.org/10.1016/j.jhydrol.2019.124533

Valley, S., Filippo, L., Pranzini, G., Puppini, U., Scardazzi, M. E., & Streetly, M. (2006). Transient flow modelling of an overexploited aquifer and simulation of artifical recharge measures. *Recharge Systems for Protecting and Enhancing Groundwater Resources*, 435–442. https://www.yumpu.com/en/document/read/28331485/recharge-systems-for-protecting-and-enhancing-groundwate

Van Huijgevoort, M. H. J., Van Lanen, H. A. J., Teuling, A. J., & Uijlenhoet, R. (2014). Identification of changes in hydrological drought characteristics from a multi-GCM driven ensemble constrained by observed discharge. *Journal of Hydrology*, *512*, 421–434. https://doi.org/10.1016/j.jhydrol.2014.02.060

van Hussen, K., van de Velde, I., Läkamp, R., van der Kooij, S., & Hekman, A. (2020). *Economische schade door droogte in 2018 | Rapport | Rijksoverheid.nl*. https://www.rijksoverheid.nl/documenten/rapporten/2019/12/18/bijlage-1-rapport-economische-schade-door-droogte-in-2018

Van Lanen, H. A. J., Prudhomme, C., Wanders, N., & Van Huijgevoort, M. H. J. (2018). Future Drought. In *Drought* (pp. 69–92). Wiley. https://doi.org/10.1002/9781119017073.ch4

Van Loon, A. F., & Van Lanen, H. A. J. (2013). Making the distinction between water scarcity and drought using an observation-modeling framework. *Water Resources Research*, *49*(3), 1483–1502. https://doi.org/10.1002/wrcr.20147

van Loon, A., Paalman, M., & Jalink, M. (2014). *Voorraadvorming door vernatten van de Stippelberg*.

van Loon, Anne F. (2015). Hydrological drought explained. *Wiley Interdisciplinary Reviews: Water*, *2*(4), 359–392. https://doi.org/10.1002/wat2.1085

Van Walsum, P. E. V, & Veldhuizen, A. A. (2011). *MetaSWAP_V7_2_0 Rapportage van activiteiten ten behoeve van certificering met Status A*. https://edepot.wur.nl/193958

Van Walsum, P. E. V, Veldhuizen, A. A., & Groenendijk, P. (2019). *SIMGRO 8.0.0 Theory and model implementation*.

Vasiliades, L., Sarailidis, G., & Loukas, A. (2017). Hydrological modelling of low flows for operational water resources management. In *European Water* (Vol. 57).

Verdonschot, P. (2010). *Het brede beekdal als klimaatbestendige buffer in de veranderende leefomgeving Flexibele toepassing van het 5B-concept in Peel en Maasvallei*. https://edepot.wur.nl/51779

Verhagen, F., Spek, T., Voortman, B., Moors, E., Querner, E., Van Den Eertwegh, G., & Van Bakel, J. (2014). Expertdialoog de Veluwe Begrijpen we het watersysteem? *STROMINGEN*, *20*(3), 5–19. https://library.wur.nl/WebQuery/wurpubs/480111

Vermeulen, P. T. M., Roelofsen, F. J., Minnema, B., Burgering, L. M. T., Verkaik, J., & Rakotonirina, D. (2019). *iMOD User Manual version 5.0*. https://oss.deltares.nl/web/imod/user-manual

Vissers, M. J. M., & van der Perk, M. (2008). The stability of groundwater flow systems in unconfined sandy aquifers in the Netherlands. *Journal of Hydrology*, *348*(3–4), 292–304. https://doi.org/10.1016/j.jhydrol.2007.10.003

Wada, Y., van Beek, L. P. H., & Bierkens, M. F. P. (2011). Modelling global water stress of the recent past: on the relative importance of trends in water demand and climate variability. *Hydrology and Earth System Sciences*, *15*(12), 3785–3808. https://doi.org/10.5194/hess-15-3785-2011

Wada, Y., van Beek, L., Wanders, N., & Bierkens, M. (2013). Human water consumption intensifies hydrological drought worldwide - IOPscience. *Environmental Research Letters*, *8*(3), 14 pp. https://doi.org/10.1088/1748-9326/8/3/034036

Wada, Yoshihide, Bierkens, M. F. P., De Roo, A., Dirmeyer, P. A., Famiglietti, J. S., Hanasaki, N., Konar, M., Liu, J., Schmied, H. M., Oki, T., Pokhrel, Y., Sivapalan, M., Troy, T. J., Van Dijk, A. I. J. M., Van Emmerik, T., Van Huijgevoort, M. H. J., Van Lanen, H. A. J., Vörösmarty, C. J., Wanders, N., & Wheater, H. (2017). Human-water interface in hydrological modelling: Current status and future directions. *Hydrology and Earth System Sciences*, *21*(8), 4169–4193. https://doi.org/10.5194/hess-21-4169-2017

Wanders, N., & Van Lanen, H. A. J. (2015). Future discharge drought across climate regions around the world modelled with a synthetic hydrological modelling approach forced by three general circulation models. *Natural Hazards and Earth System Sciences*, *15*(3), 487–504. https://doi.org/10.5194/nhess-15-487-2015

Wanders, N., Wada, Y., & Lanen, H. A. J. Van. (2015). Global hydrological droughts in the 21st century under a changing hydrological regime. *Earth Syst. Dynam*, *6*, 1–15. https://doi.org/10.5194/esd-6-1-2015

Wendt, D., Scanlon, B., & Loon, A. Van. (2018). Examining management interventions on hydrological droughts. *Geophysical Research Abstracts*, *20*(2), 2018–16887. https://ui.adsabs.harvard.edu/abs/2018EGUGA..2016887W/abstract

Wesselingh, F. (n.d.). *Zandlandschap - Geologie van Nederland*. Naturalis. Retrieved March 16, 2020, from https://www.geologievannederland.nl/landschap/landschappen/zandlandschap

Wiel, K., Wanders, N., Selten, F. M., & Bierkens, M. F. P. (2019). Added Value of Large Ensemble Simulations for Assessing Extreme River Discharge in a 2 °C Warmer World. *Geophysical Research Letters*, *46*(4), 2093–2102. https://doi.org/10.1029/2019GL081967

Wilhite, D. (2005). *Drought and water crises*. Taylor & Francis. https://s3.amazonaws.com/academia.edu.documents/50870703/Drought_monitoring_New_tools_for_the_21s20161213-26734-e5omat.pdf?response-content-disposition=inline%3B filename%3DDrought_monitoring_New_tools_for_the_21s.pdf&X-Amz-Algorithm=AWS4-HMAC-SHA256&X-Am

Wösten, H., De Vries, F., Hoogland, T., Massop, H. T. L., Veldhuizen, A. A., Vroon, H., Wesseling, J., Heijkers, J., & Bolman, A. (2013). BOFEK2012, de nieuwe, bodemfysische schematisatie van Nederland. In *Alterra report* (Vol. 2387). http://edepot.wur.nl/247678

Zuurbier, K. G., Kooiman, J. W., Groen, M. M. A., Maas, B., & Stuyfzand, P. J. (2015). Enabling Successful Aquifer Storage and Recovery of Freshwater Using Horizontal Directional Drilled Wells in Coastal Aquifers. *Journal of Hydrologic Engineering*, *20*(3), B4014003. https://doi.org/10.1061/(ASCE)HE.1943-5584.0000990

Appendices

Appendix A – Comparison between the groundwater levels at 80% occurrence frequency (left) and mean groundwater levels (right) considering all 30 years of the model run (no spin up) and only from 01-01-1993 onwards (spin up)

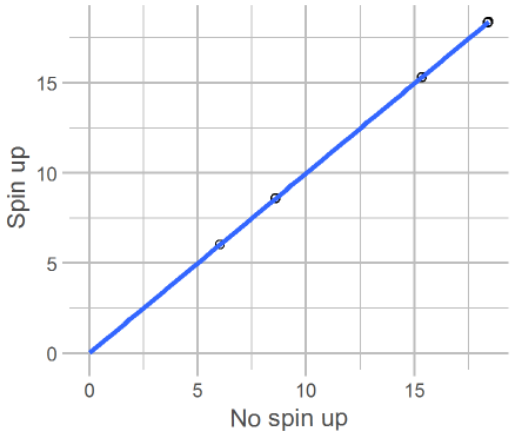

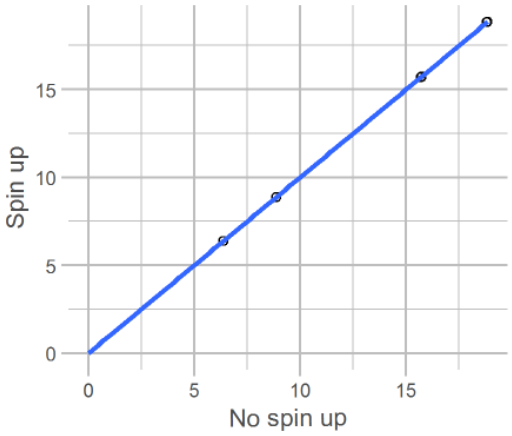

Appendix B – Time series of the monthly averages of the groundwater levels of the baseline scenario at each observation well

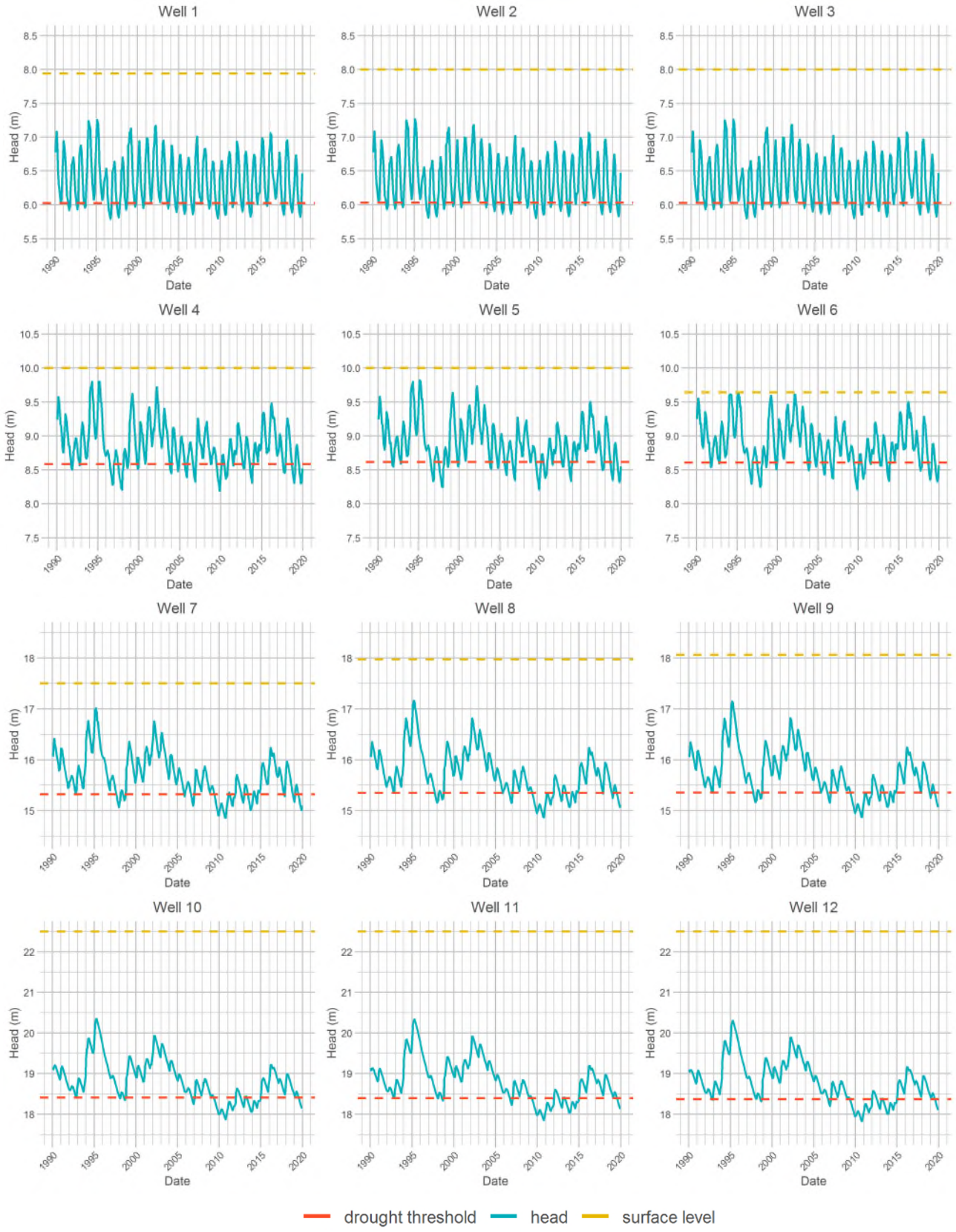

Appendix C – Time series of the monthly averages of groundwater contribution to the river for the baseline model simulation compared to the value of the 30 year mean contribution value

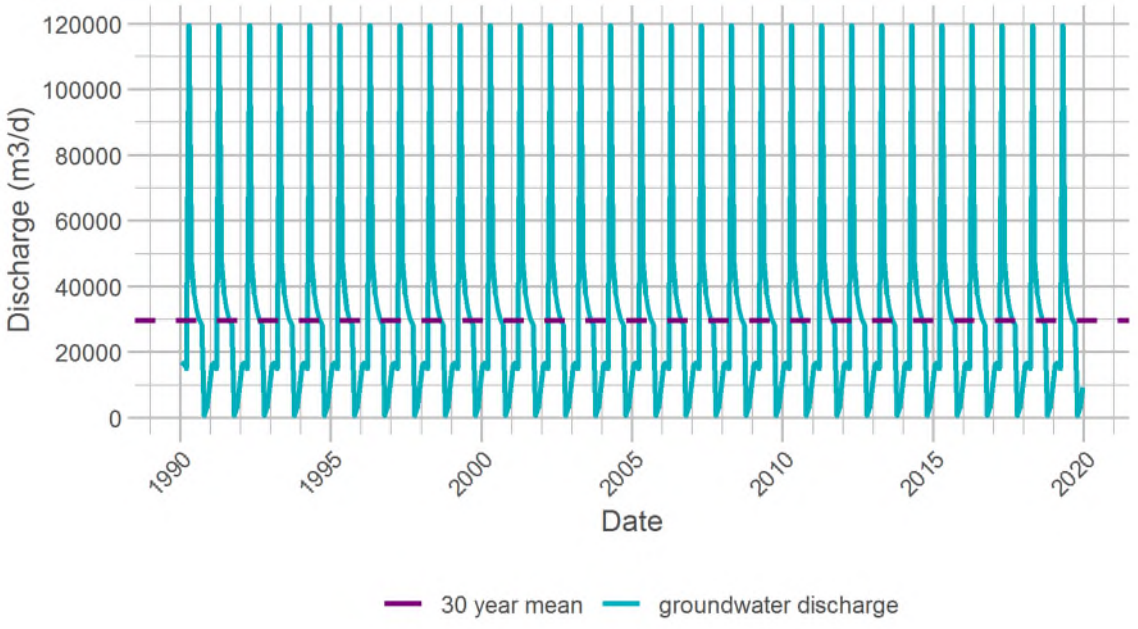

Appendix D – Time series of atmospheric water balance components.

The values shown are precipitation (P) and reference evapotranspiration (ET) from KNMI data (model input), as well as bare soil evaporation (Ebs), vegetation interception evaporation (Eic), evaporation due to ponding (Ebs) actual transpiration (Tact), actual evapotranspiration (Eact) and potential transpiration (Tpot) obtained from MetaSWAP.

Appendix E – Pressure heads and Relative transpiration of all observation well locations

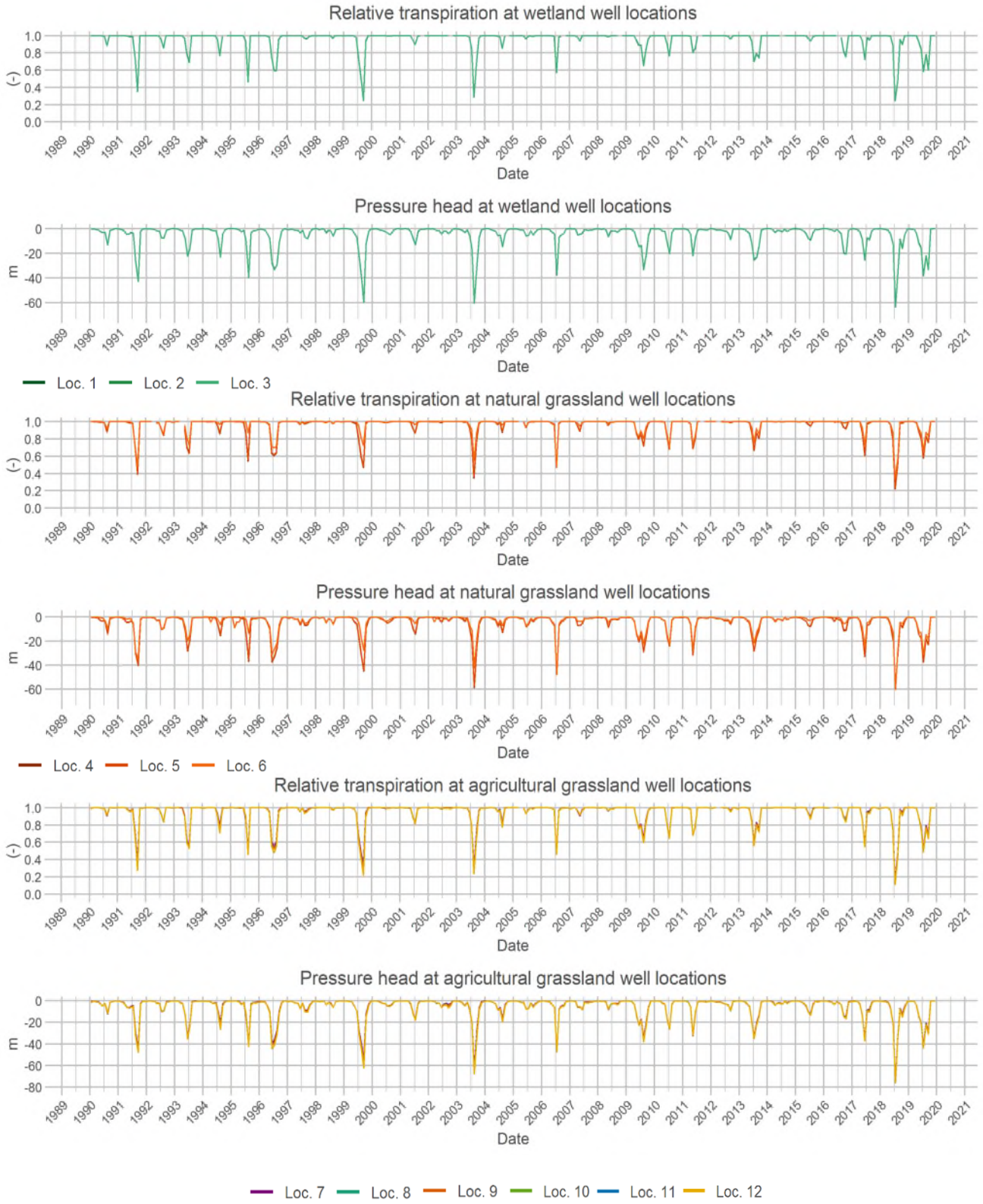

Appendix F - Mean monthly values of the surface runoff, infiltration, and groundwater recharge MetaSWAP results of the baseline scenario. Negative values of runoff represent water arriving at the cell from uphill, while negative values of recharge represent water moving from the saturated zone to the unsaturated zone.

Appendix G – Time series comparing groundwater levels of all MAR and Baseline scenarios in each observation well.

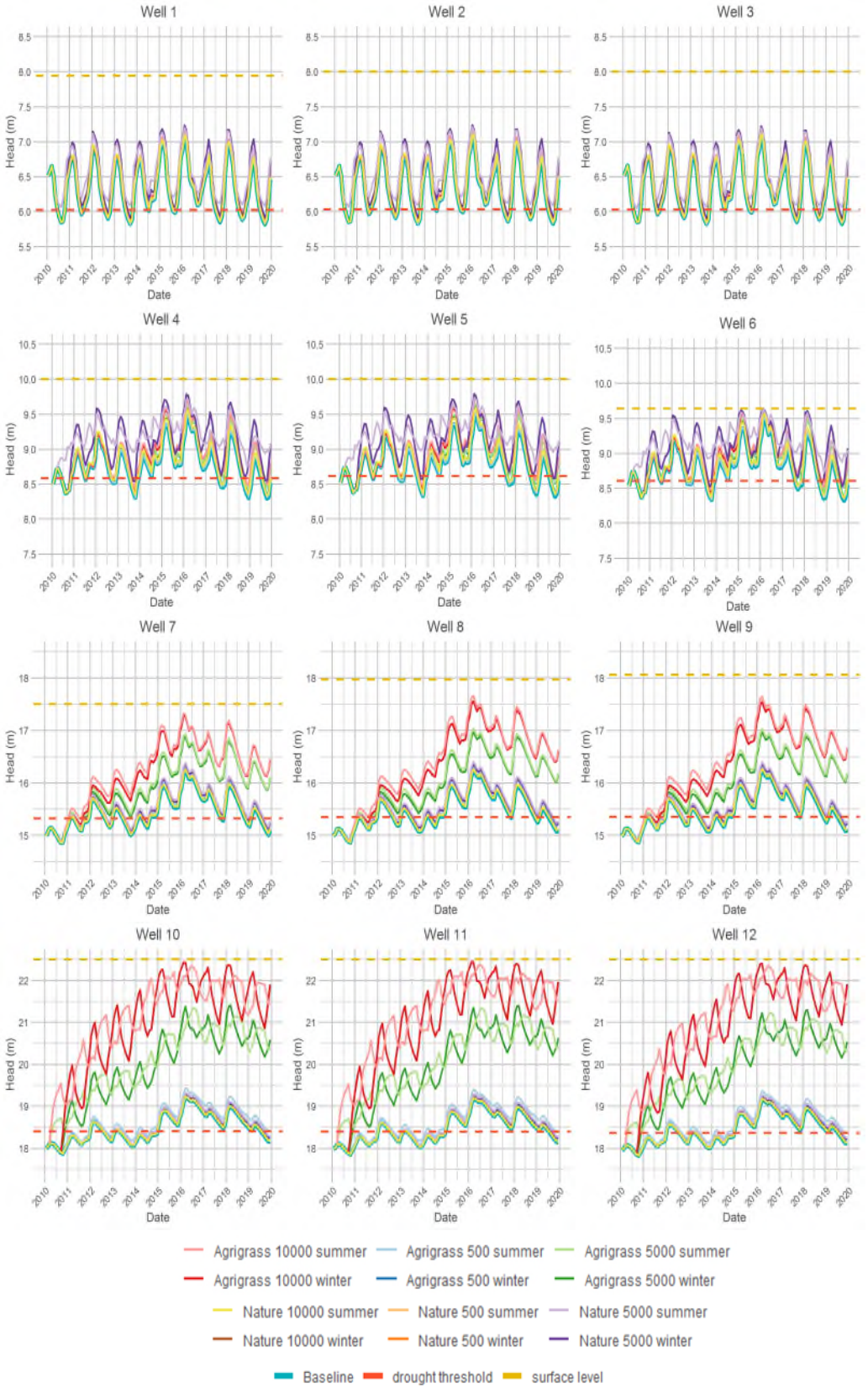

Appendix H – Top : Maps showing the difference in groundwater levels between the winter and summer applications of AG MAR 5000 (a), AG MAR 10000 (b), N MAR 5000 (c) and N MAR 10000 (d). Bottom: Maps showing the difference in soil moisture pressure heads between the winter and summer applications of AG MAR 5000 (e), AG MAR 10000 (f), N MAR 5000 (g) and N MAR 10000 (h).

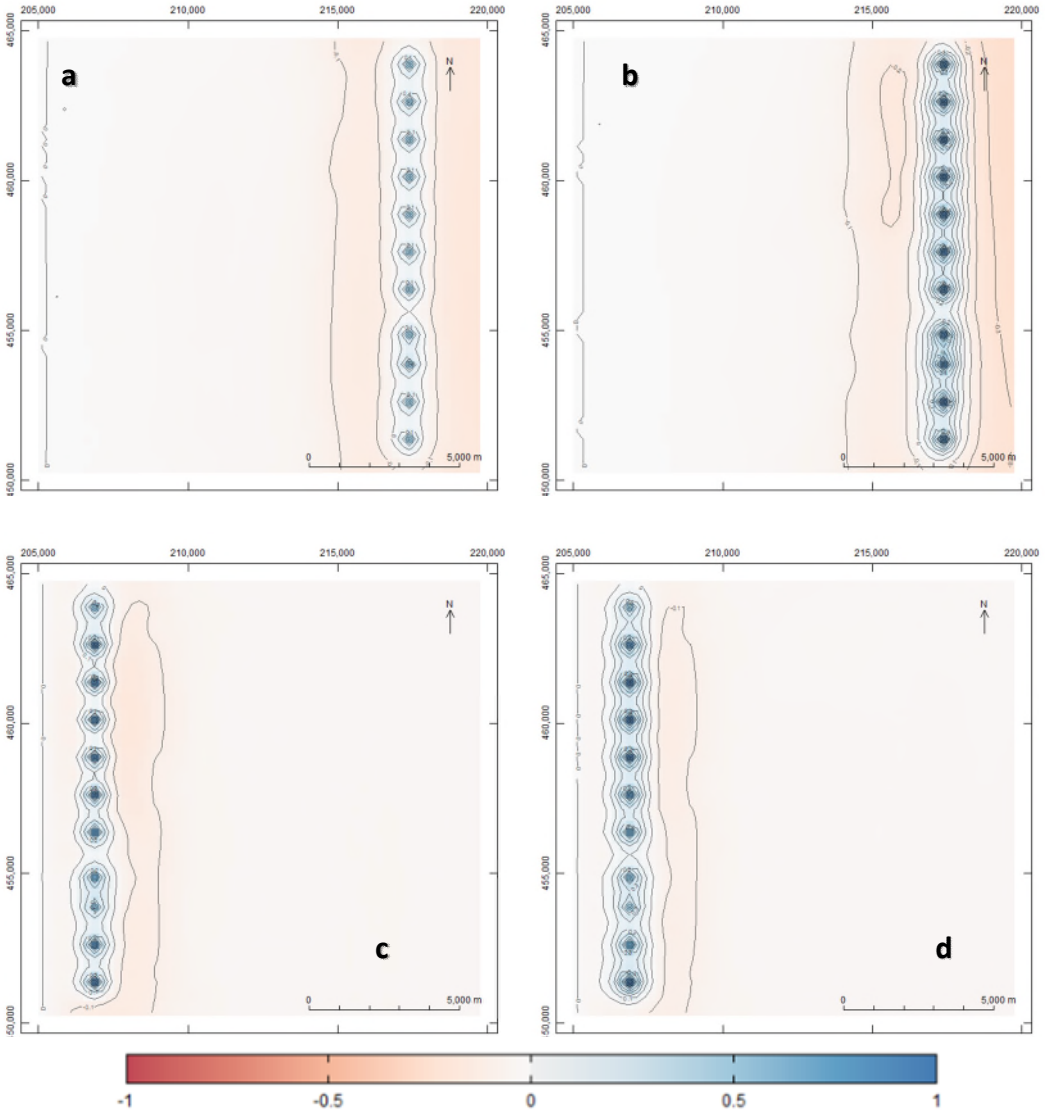

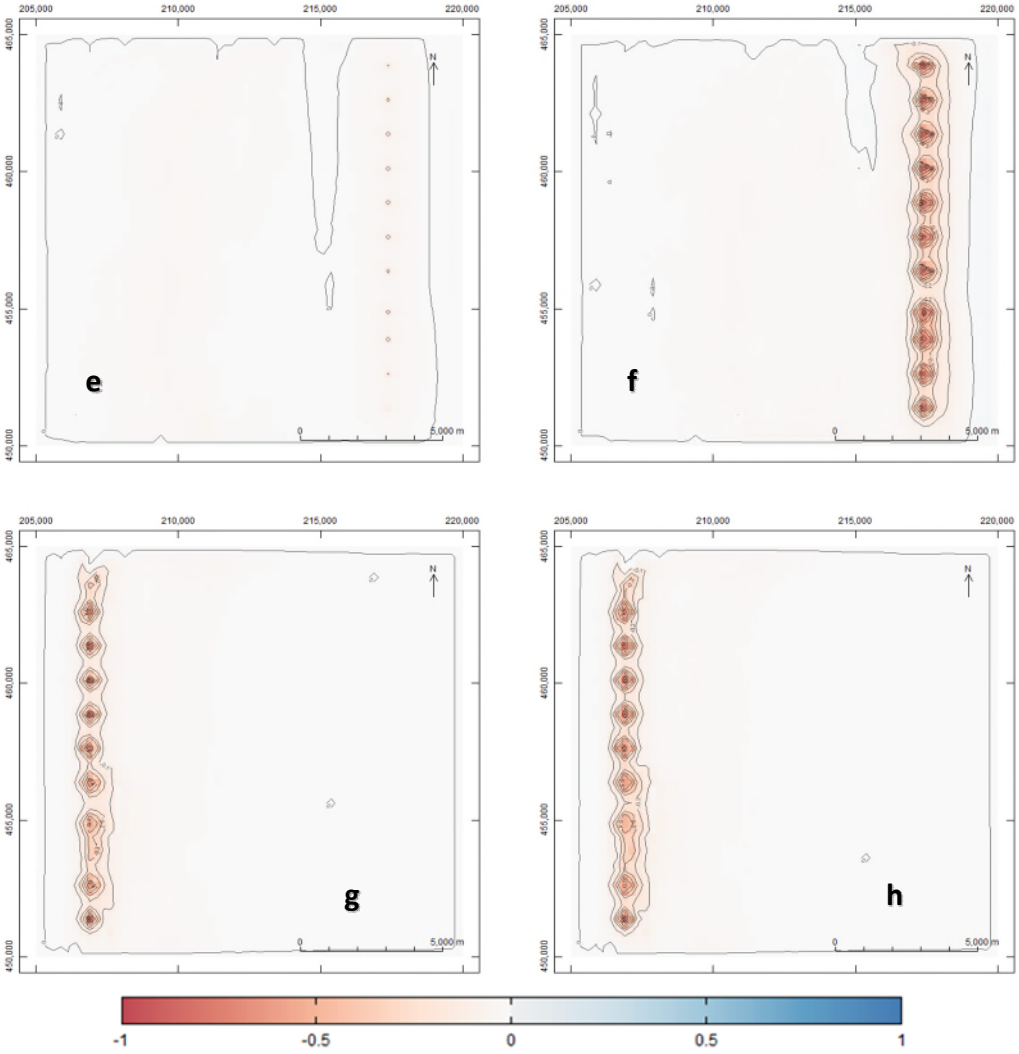
205,000
210,000
215,000
220,000
465,000
460,000
455,000
450,000
N
e
f
g
h
0
5,000 m
-1
-0.5
0
0.5
1

Appendix I - Differences between each MAR scenario and the baseline of the relative transpiration and pressure heads in the root zone at each well location. Note: each column belongs to the well location given in the first row of graphs.


Relative transpiration change at natural grassland well locations
Loc. 4
Loc. 5
Loc. 6
(-)
Date
Relative transpiration change at natural grassland well locations
(-)
Date
Pressure head change at natural grassland well locations
m
Date
Pressure head change at natural grassland well locations
m
Date
Agrigrass 10000 summer
Agrigrass 500 summer
Agrigrass 5000 summer
Agrigrass 10000 winter
Agrigrass 500 winter
Agrigrass 5000 winter
Nature 10000 summer
Nature 500 summer
Nature 5000 summer
Nature 10000 winter
Nature 500 winter
Nature 5000 winter

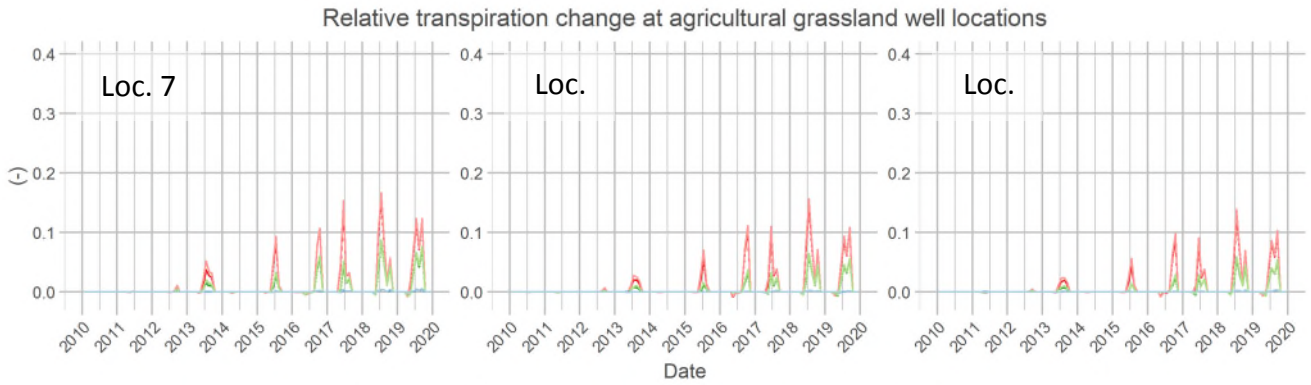
Relative transpiration change at agricultural grassland well locations
Loc. 7
Loc.
Loc.
(-)
Date

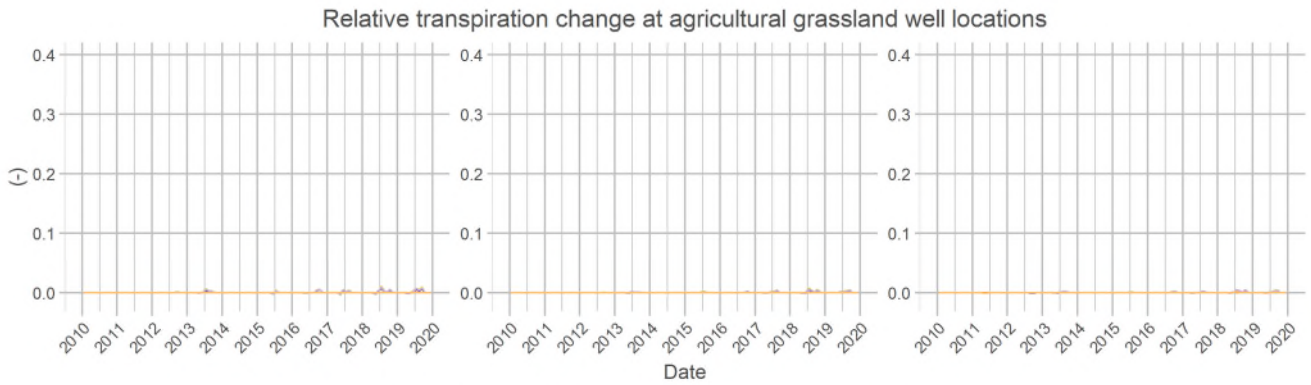
Relative transpiration change at agricultural grassland well locations
(-)
Date

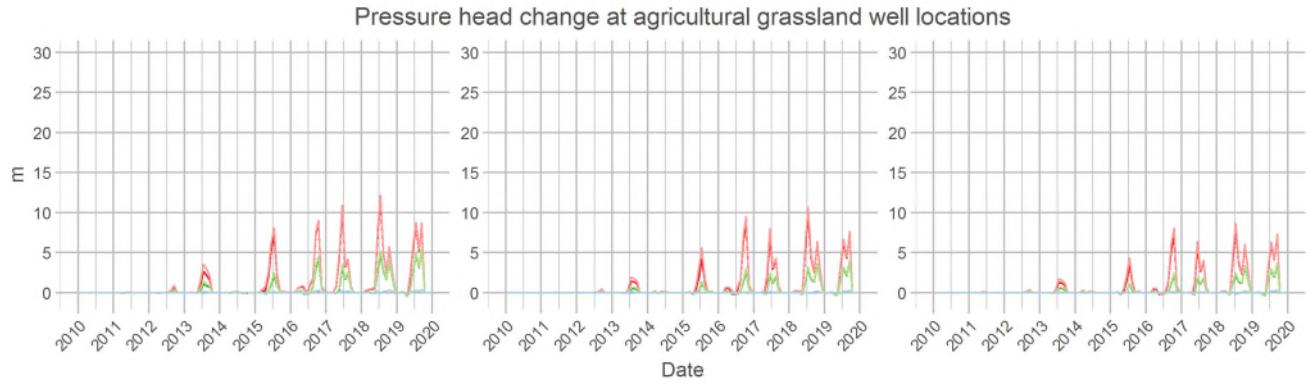
Pressure head change at agricultural grassland well locations
m
Date

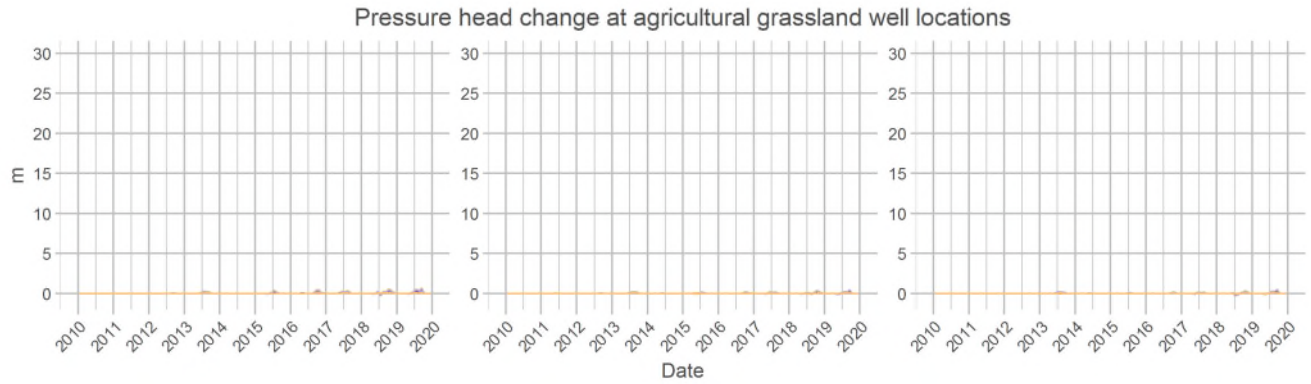
Pressure head change at agricultural grassland well locations
m
Date


Agrigrass 10000 summer
Agrigrass 500 summer
Agrigrass 5000 summer
Agrigrass 10000 winter
Agrigrass 500 winter
Agrigrass 5000 winter
Nature 10000 summer
Nature 500 summer
Nature 5000 summer
Nature 10000 winter
Nature 500 winter
Nature 5000 winter

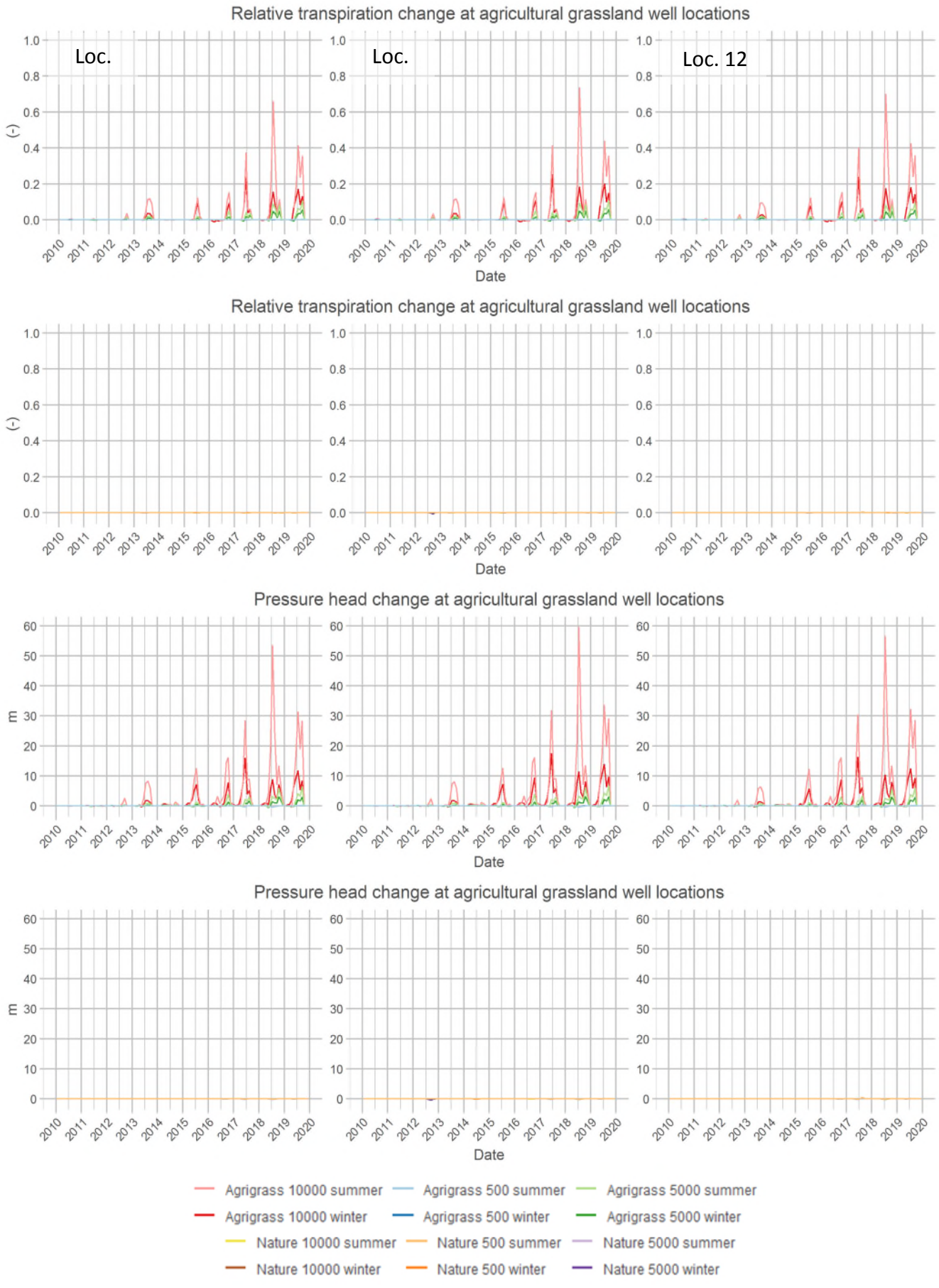
Relative transpiration change at agricultural grassland well locations
Loc.
Loc.
Loc. 12
(-)
Date
Relative transpiration change at agricultural grassland well locations
(-)
Date
Pressure head change at agricultural grassland well locations
m
Date
Pressure head change at agricultural grassland well locations
m
Date
Agrigrass 10000 summer
Agrigrass 500 summer
Agrigrass 5000 summer
Agrigrass 10000 winter
Agrigrass 500 winter
Agrigrass 5000 winter
Nature 10000 summer
Nature 500 summer
Nature 5000 summer
Nature 10000 winter
Nature 500 winter
Nature 5000 winter